Water Resources Research

RESEARCH ARTICLE
10.1029/2017WR022304

Age-Ranked Storage-Discharge Relations: A Unified Description of Spatially Lumped Flow and Water Age in Hydrologic Systems

C. J. Harman[1,2]

[1]Department of Environmental Health and Engineering, Johns Hopkins University, Baltimore, MD, USA, [2]Department of Earth and Planetary Science, Johns Hopkins University, Baltimore, MD, USA

Key Points:
- Storage-discharge relations and transit time distributions are unified in a single relationship capturing both celerity and velocity effects
- Empirical data and theory suggest old water release may be accelerated or suppressed at high discharge or catchments wetness
- Robust inferences about oldest water turnover require new approaches to functional estimation with age-dependent uncertainty

Correspondence to:
C. J. Harman,
charman1@jhu.edu

Citation:
Harman, C. J. (2019). Age-ranked storage-discharge relations: A unified description of spatially lumped flow and water age in hydrologic systems. *Water Resources Research*, *55*, 7143–7165. https://doi.org/10.1029/2017WR022304

Received 27 NOV 2017
Accepted 1 JUL 2019
Accepted article online 6 JUL 2019
Published online 23 AUG 2019

Abstract A storage-discharge relation tells us how discharge will change when new water enters a hydrologic system but not which water is released. Does an incremental increase in discharge come from faster turnover of older water already in storage? Or are the recent inputs rapidly delivered to the outlet, "short-circuiting" the bulk of the system? Here I demonstrate that the concepts of storage-discharge relationships and transit time distributions can be unified into a single relationship that can usefully address these questions: the age-ranked storage-discharge relation. This relationship captures how changes in total discharge arise from changes in the turnover rate of younger and older water in storage and provides a window into both the celerity and velocity of water in a catchment. This leads naturally to a distinction between cases where an increase in total discharge is accompanied by an increase (old water acceleration), no change (old water steadiness), or a decrease in the rate of discharge of older water in storage (old water suppression). The simple theoretical case of a power law age-ranked storage-discharge relations is explored to illustrate these cases. Example applications to data suggest that the apparent presence of old water acceleration or suppression is sensitive to the functional form chosen to fit to the data, making it difficult to draw decisive conclusions. This suggests new methods are needed that do not require a functional form to be chosen and provide age-dependent uncertainty bounds.

1. Introduction

1.1. A Motivating Question About Discharge Across the Age Distribution

A significant advance in surface water hydrology over the last several decades has been the widespread observation that the stream discharge released by a headwater catchment in response to a storm may not be entirely (or even mostly) made up of water that fell during that storm (Kirchner, 2003; McDonnell et al., 2010; McGuire & McDonnell, 2006; Neal & Rosier, 1990; Sklash & Farvolden, 1979). Rather, event hydrographs are often composed of older water stored in the catchment from previous storms, only now driven into the stream as a result of the increased potential energy contributed by the addition of new water, and the activation of new flow paths (Klaus & McDonnell, 2013).

Recently, an additional pattern has been identified: Many catchments tend to preferentially release younger water under wetter conditions (Benettin et al., 2015, 2017; Birkel & Soulsby, 2016; Birkel et al., 2015; Harman, 2015; Hrachowitz et al., 2013; Klaus et al., 2015; Remondi et al., 2018; Rodriguez et al., 2018; Soulsby et al., 2015; Tunaley et al., 2017; van Huijgevoort et al., 2016; Yang et al., 2018). This has been termed the "inverse storage effect" because it runs counter to the behavior that would be expected if catchments were a single well-mixed store (in which greater storage would result in a smaller contribution of the youngest water; Harman, 2015).

This paper discusses a more general question: *How does the discharge of water of different ages change when there is a change in the overall discharge?* While the derivations and examples developed here focus on discharge, the framework proposed can equally apply to evapotranspiration or other fluxes out of the system. We are interested particularly in the absolute changes, rather than the relative contributions to the total, since the absolute changes *cause* the total discharge to change. When storm or snowmelt inputs induce changes in the release of water of different ages, the sum of those changes *is* the change in total discharge.

This shift in perspective is helpful for thinking about how time-variable age structure arises. In catchments that exhibit an inverse storage effect in the age-structure of discharge, for example, the effect might arise in

several different ways: (i) It may be purely because of an enhanced release of younger water, (ii) the discharge of older water may also increase, just not as much as younger water, or (iii) the release of older water may in fact decline, suppressed in some way by the processes that are preferentially delivering younger water. All three are physically plausible in a catchment. Additional potential energy may pressurize the saturated zone, increasing discharge of older water. It may bypass the existing storage and have no effect on the release of older water. Or groundwater ridging at the hillslope base may generate adverse gradients at the hillslope toe (Zimmer & McGlynn, 2017), perhaps reducing the discharge of older water.

This fundamental question has a bearing on more applied problems, such as how long it takes for excess nitrate leaching from agricultural soils to reach receiving water bodies and how long it would take for the efforts at mitigation to show up as reduced nitrate loads (Meals et al., 2010; Van Meter & Basu, 2015). Would a change in hydroclimate result in an increase or a decrease in the time required to "flush" the landscape (e.g., Wilusz et al., 2017)?

But it can also be seen as a test of our basic understanding and of the tools we use to construct that understanding (i.e., models). What does the available data allow us to say about the release of water of different ages from storage, and do our models agree? This paper does not suppose to have a complete answer to this question, but I do want to suggest a framework for asking the question in a way that leads (hopefully) to useful answers.

1.2. Celerity and Velocity in Hydrologic Systems

The question above could be framed in terms of the relationship between the *celerity* of a catchment's hydrologic response to water inputs and the *velocity* of the water molecules that make up that response (McDonnell & Beven, 2014). Celerity, broadly speaking, is the rate additional potential energy supplied by water inputs propagates through the landscape and ultimately does the work of mobilizing water into the stream and out of the watershed. Thus, celerity determines how quickly the stream responds to the storm and how long it takes for discharge to decline after the storm. Velocity, on the other hand, determines how long it takes water molecules to traverse the watershed and so controls the age composition of discharge.

Celerity and velocity are controlled by different mechanisms; in particular, they have distinct relationships to storage. As McDonnell and Beven (2014) point out, velocity is controlled by the rate of flow at the pore scale, which is determined by the total flux of water and the total volume that flux is turning over. Celerity, on the other hand, is often controlled by the amount of water required to fill storage deficits and raise the water table (and thus the water potential of hydraulically connected water), as well as the amount of water that must be released through lateral flow in order to lower water tables again. The former is typically significantly larger than the latter (McDonnell & Beven, 2014), and so celerity in watersheds is typically many times faster than the velocity. Since the "wave" of energy (i.e., hydraulic head) moves ahead of the molecules of water it arrived with, the water ultimately mobilized into the stream as discharge is *necessarily* partly made up of water that was already in the watershed.

Despite their differences, velocity and celerity are intimately related to one another in catchments. The energy being transmitted (at the rate described by the celerity) is also the energy that is accelerating the velocity of pore water and being lost to heat through viscosity. The question posed in this paper is about the nature of that relationship. Parcels of water that take a long time to travel through the catchment (thus having an apparently slow velocity) might have a slow celerity, resulting in a slow, steady rate of discharge, or they might have a fast celerity, making small, brief "jumps" each time it rains (but yielding a slow rate of discharge when averaged over time).

For a variety of reasons, landscape units like watersheds, hillslopes, and stream reaches are often examined and modeled as integrated wholes (Sivapalan, 2005). The integration of these flow systems into (roughly) equivalent "lumped" units prevents consideration of length scales explicitly. The heterogeneity and spatiotemporal variability that produces a (changing) distribution of velocities and celerities have been integrated out of the picture. This makes it difficult to sensibly talk about a length/time ratio like celerity and velocity.

It would be helpful to have a framework of well-defined corresponding quantities that can be applied in lumped systems. In fact, these already exist as the *transit time* and *hydraulic response time*. The transit time is simply the time taken for a parcel of water to move through the system from input (e.g., as precipitation) to output (e.g., as discharge or ET) and so is a lumped measure of the velocity. The hydraulic response time

can be understood as the time taken for a perturbation in the inputs (i.e., some impulse of precipitation or recharge) to propagate through the system and ultimately produce a perturbation in the output (i.e., a hydrograph peak). Both transit time and hydraulic response time are not single quantities for a given catchment (or for a given moment in time) but rather must be represented by distributions (which may vary in time). We will discuss transit time distributions (TTDs) shortly. The distribution of hydraulic response times can be represented by the instantaneous unit hydrograph (the impulse response function) in a linear model. But what about for a nonlinear storage-discharge relationship? And how are TTDs and hydraulic response times related to each other? As we shall see, it is more natural to address these questions by considering the relationship to storage, rather than to age or time itself.

1.3. Fundamental Quantities: Storage, Discharge, and Age

Here I propose a framework for representing the dynamics of storage, discharge, and age in a way that addresses many of the issues raised above. I propose to combine (or at least set side-by-side) well-studied approaches to understanding relationships between storage and discharge (e.g., the catchment sensitivity functions of; Kirchner, 2009) with the StorAge Selection (SAS) approach to identifying *which* water (in terms of age) is release from storage (Botter et al., 2011; Harman, 2015; van der Velde et al., 2012). The major elements of this framework are not new, though the way they are combined and arranged is. I will argue that when SAS and storage-discharge dynamics are combined, they are in a sense "greater than the sum of their parts": They allow new insights to be obtained that are obscure when discharge and SAS functions are considered separately. They reveal how changes in discharge are accommodated by changes in the turnover of storage of different ages. Simultaneously, they reveal the converse: How changes in the age distribution of discharge arise from changes in rate of discharge of older and younger water from the catchment.

In its most basic form, this framework is simply a way of unifying information about hydrologic storage, discharge, and water age. Where data suggest that the time variability of flow and transport (celerity and velocity) are indeed tightly coupled to storage, the implications of this coupling for the release of water of different ages can also be examined. It can therefore be useful for examining data obtained directly from observations (Kim et al., 2016; Harman & Kim, 2014), a 3-D spatially distributed particle-tracking model (Danesh-Yazdi et al., 2018) or a lumped conceptual model (Benettin et al., 2015; Hrachowitz et al., 2013).

The relationship between storage and discharge is at the heart of many descriptions of catchment hydrological behavior (Beven, 2012). This relationship may be tightly captured by some 1-to-1 storage-discharge relationship or catchment sensitivity function (Kirchner, 2009), or it may be highly hysteretic, particularly when parts of the catchment connect and disconnect in complex ways (e.g., Spence, 2010, and see Beven, 2006). Either way, it represents a fundamental expression of the hydrologic dynamics of a watershed. A variety of methods have been developed to extract storage-discharge relationships empirically from analysis of observed hydrographs (particularly recession curves), in order to gain insight into catchment function (Wittenberg, 1999; Wittenberg & Sivapalan, 1999), and attempt to infer physical properties of the watershed (Brutsaert & Nieber, 1977; Dralle et al., 2017).

SAS functions are a generalization of TTDs to time-variable flow systems. A TTD is the distribution of ages that parcels of water attain as they exit the system, measured from the time they first entered (e.g., as rainfall or snowmelt into a catchment). SAS was developed to capture the time variability of TTD in a rigorous mathematical framework (Botter et al., 2011; Harman, 2015; van der Velde et al., 2012). The SAS functions themselves are probability distributions over the storage "ranked" by age (Harman, 2015) describing the relative contribution of each "age-ranked storage" to discharge.

Although both S-Q relations and transit time analysis address fundamental relationships between storage and discharge, the application of TTD and SAS has been largely disconnected from consideration of storage-discharge relations and the associated recession curve analysis methods. As demonstrated below, these conceptual tools can be easily unified into a single family of functional relationships. No new assumptions are needed to unify SAS functions and storage-discharge relations—doing so is actually quite trivial.

The resulting framework provides an elegant way to examine whether changes in discharge resulting from a precipitation event are associated with an increase, decrease, or no change in the rate of discharge of older water present in the catchment prior to the event. This allows us to make some more precise statements about the relationship between velocity and celerity in lumped hydrologic systems.

This framework is be elaborated below, along with a number of theoretical derivatives. Application of the framework is demonstrated using data from two case studies that appear in Harman (2015) and Harman et al. (2016). Finally, some lessons and further research needs are discussed.

2. Theoretical Foundations of Age-Ranked Storage-Discharge Relationships

2.1. Storage and Storage-Discharge Relations

The storage of water in a watershed (or some subcompartment of a watershed, like the saturated groundwater zone) is determined by conservation of mass, which requires that the sum of input minus output fluxes equal the change in storage over time. For instance,

$$\frac{dS}{dt} = J - Q - E, \tag{1}$$

where J is the precipitation rate and Q and E are the rates of discharge and evapotranspiration, respectively. All the variables (S, J, Q, and E) are typically assumed to be spatially averaged over the watershed and vary only in time. Note that even with perfect knowledge of these fluxes, the conservation law cannot be solved to give the total storage in a system, only the storage relative to some reference state $\Delta S = S - S_{\text{ref}}$.

A storage-discharge relationship is the assertion that the rate of discharge has some functional dependence on storage:

$$Q = f(\Delta S). \tag{2}$$

This relationship parameterizes the Q term in the conservation equation, allowing it to be solved once data or some other parameterizations are provided for J and E. When used as model components, such relationships are most commonly used to approximate streamflow released from groundwater (Wittenberg, 1999), at scales where time delays due to routing along the river network can be neglected and at times and places where connectivity is high or the landscape connects and disconnects in a consistent way. The catchment sensitivity function $g(Q)$ was proposed by Kirchner (2009) as an alternative form of storage-discharge relations:

$$\frac{dQ}{dS} = f'(f^{-1}(Q)) = g(Q), \tag{3}$$

where f' is the derivative of f and $\Delta S = f^{-1}(Q)$ is the inverse function. Note that g encodes essentially the same information and assumptions as f but differs from f in two ways: It is the derivative, and it is expressed in terms of the discharge, rather than the storage.

Even where Q does not have consistent relationship to the storage ΔS that appears in the water balance, it may be possible to extract storage-discharge relationships from recession analysis (Brutsaert & Nieber, 1977; Wittenberg & Sivapalan, 1999). Dralle et al. (2018) recently showed how these can be combined with estimates of ΔS (obtained by integrating the water balance components directly) to decompose catchment storage into hydraulically connected and disconnected components and related these to observed water storage and runoff generation processes.

2.2. Storage and Storage-Discharge Relations as a Measure of Celerity

It seems reasonable to equate "celerity" in lumped hydrologic systems as the rate a perturbation in the inputs (i.e., some impulse of precipitation or recharge) propagates through the system and ultimately produces a perturbation in the output (i.e., a peak in the hydrograph) and the hydraulic response time as the time required for this propagation. The physical processes underlying the propagation of a perturbation are captured by storage-discharge and catchment sensitivity functions in certain cases. In analytical solutions relating storage-discharge relationships to physical principles like Darcy's Law, storage is explicitly used as a proxy for the potential energy gradient driving flow (Harman & Sivapalan, 2009; Troch & De Troch, 1993; Troch et al., 2003) and a master variable controlling the aggregate resistance along the connected flow paths available to dissipate that gradient (Lehmann et al., 2007; Rupp & Selker, 2005). Viewed this way, the hydraulically connected storage obtained by Dralle et al. (2018) from integration of $g(Q)$ can be seen as the volume of storage deficit that must be drained to decrease the potential gradients and hydraulic connectivity such that discharge decreases by a given amount.

Therefore, there ought to be a way to extract a measure of the celerity and hydraulic response time scale from the storage-discharge relationship itself. Where a storage-discharge relation holds, the effect of such a

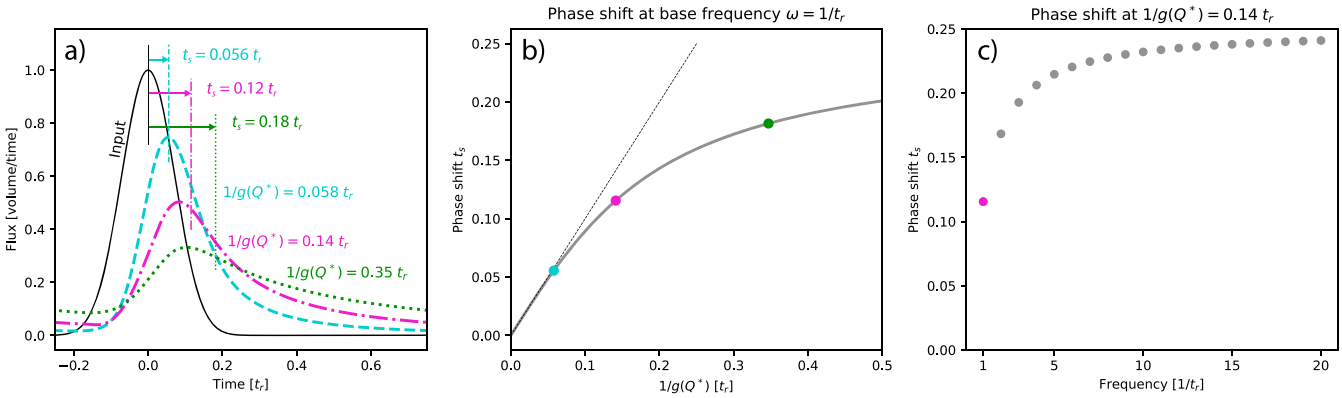

Figure 1. (a) Illustration of the way a storage-discharge relationship can be related to the concept of celerity using the idealized example of discharge response to periodic inputs (black line) for simple power law storage-discharge relations like (27) with $b = 1.5$, $Q_0 = 1$, and $s = 0.05$ (cyan), $s = 0.1$ (magenta), and $s = 0.2$ (green). The phase shift t_s at the base frequency $\omega = 1/t_r$ is given for each case, along with the value of $1/g(Q^*)$ (with Q^* evaluated at the output hydrograph peak). For small values of $1/g(Q^*)$, this value closely approximates the phase shift, justifying its interpretation as the hydraulic response times, and characteristic of the celerity of a lumped hydrologic system. Details are given in Appendix A. (b) The phase shift at the base frequency as a function of $1/g(Q^*)$, showing how the periodicity of the forcing ion this simple example limits the size of the time delay that can be induced by a given $1/g(Q^*)$. (c) Phase shift as a function of frequency for a fixed $1/g(Q^*)$, showing that higher-frequency components of the inputs undergo a larger phase shift in the outputs—this changes the shape of the output hydrograph.

perturbation will decay in the outflow at a rate that depends on $g(Q)$, which has units of 1/time. In fact, when $g(Q)$ is constant, the decay is exponential with an e-folding time of exactly $1/g(Q)$. Otherwise, the decay rate must vary in time (Kirchner, 2009). This suggests we might equate the (time varying) hydraulic response time with the time scale $1/g(Q)$.

This idea can be demonstrated more precisely using spectral analysis. If we linearize $g(Q)$ around some characteristic discharge Q^*, we can solve the resulting model in the spectral domain (see Appendix A for details). The nonlinear model and results of spectral analysis are illustrated in Figure 1. It can be shown that for periodic inputs (with period t_r), the phase shift t_s between the inputs and outputs at the base frequency $\omega = 1/t_r$ can be approximated by

$$t_s \approx 1/g(Q^*). \tag{4}$$

In other words, under appropriate conditions, the time scale given by $1/g(Q)$ closely approximates the delay between a fluctuation in the inputs and a fluctuation in the outputs. Of course, the situation is made more complex by the presence of multiple frequencies in the input signal (higher frequencies experience larger phase shifts) and the nonlinearity of the storage-discharge relationship. Despite these complications, it is clear that $1/g(Q)$ is characteristic of the hydraulic response time of the system, which has the same relationship to the celerity through the lumped system as the transit time has to the velocity.

Note that the derivations below do not assume or require the existence of a tight storage-discharge relation unless stated explicitly.

2.3. Age-Ranked Storage and Discharge and Their Complements

The SAS approach to understanding water age dynamics is also built on an expression of conservation of mass, but one generalized to consider changes in the storage of water of different ages. The age-ranked storage $S_T(T, t)$ is the volume of water in storage that is younger than age T at time t. Similarly, the age-ranked discharge $Q_T(T, t)$ is the rate that water younger than T is leaving the catchment as discharge at time t. Note that for $T = 0$, $S_T = 0$ and $Q_T = 0$.

The conservation law for age-ranked storage is given by (Botter et al., 2011; Harman, 2015; van der Velde et al., 2012):

$$\frac{\partial S_T}{\partial t} + \frac{\partial S_T}{\partial T} = J - Q_T - E_T. \tag{5}$$

As with equation (1), data or parameterizations of Q_T and E_T must be provided in order to solve the equation. A SAS function Ω_Q is a (possibly time-varying) function that provides this. It is normalized by the total

discharge, so

$$Q_T = Q(t)\,\Omega_Q(S_T, t). \tag{6}$$

The function Ω has the properties of a cumulative probability distribution function over S_T and can be parameterized using any appropriate distribution. A uniform distribution reproduces the behavior of a well-mixed system, but other distributions, such as a gamma distribution, can also be used (Harman, 2015).

It is useful to also consider complementary quantities that represent the storage and discharge of water *older* than age T:

$$\overline{Q_T}(T, t) = Q(t) - Q_T(T, t), \tag{7}$$

$$\overline{S_T}(T, t) = S(t) - S_T(T, t). \tag{8}$$

Since it is not possible to know S, only ΔS, it is more useful to replace the latter definition with a similar sort of relative storage:

$$\Delta\overline{S_T}(T, t) = \Delta S(t) - S_T(T, t) \tag{9}$$

$$= \overline{S_T}(T, t) - S_{\text{ref}}. \tag{10}$$

Note that for $T = 0$, $\Delta\overline{S_T} = \Delta S$ and $\overline{Q_T} = Q$. Figure 2 provides a visualization of these quantities and their relationships to one another.

The quantities Q_T and S_T and their complements $\overline{Q_T}$ and $\Delta\overline{S_T}$ differ in an important way. Consider how they change when new water is added to the system, but its additional potential energy is not added to the potential energy of the existing water in storage, and it does not modify the connectivity or aggregate resistance to flow anywhere. This might be the case for a small storm over a forested catchment that is mostly captured by canopy interception. In this case the values of $\Delta\overline{S_T}$ and $\overline{Q_T}$ for older water in storage are not affected by the additional new water. Nor does Q_T have to change, since the rate of discharge younger than any particular age has not changed. However, the values of S_T associated with every parcel of water in the system do change, since the intercepted water is now the youngest water in the system. This means that the relationship between S_T and Q_T (discussed in the next section) must also change.

2.4. Age-Ranked Storage-Discharge Relations

In previous applications of the SAS approach, it has been typical to consider discharge Q and the SAS function Ω separately. A central purpose of this paper is to demonstrate that insights can come from considering them together as a whole—insights that are obscure when they are only considered apart.

One way of considering them together is illustrated in Figure 2, which shows the relationship between $\Delta\overline{S_T}$ and $\overline{Q_T}$ implied by equations (6)–(9). The blue curve is simply the SAS function Ω but rotated a half turn and scaled vertically by the discharge. We will call this curve the *age-ranked storage-discharge relation* f_T defined by

$$\overline{Q_T} = f_T(\Delta\overline{S_T}, t). \tag{11}$$

From the definitions above, this curve is related to the discharge and SAS function by

$$f_T(\Delta\overline{S_T}, t) = Q(t)\left(1 - \Omega(\Delta S(t) - \Delta\overline{S_T}, t)\right). \tag{12}$$

An example of this function is illustrated in Figure 2. The colored bar along the horizontal storage axis represents the age-ranked storage in a watershed. Each colored interval represents an identical volume of storage, and the total length of the bar represents the total volume. These volumes are arranged with the youngest on the right and the oldest on the left. The colored bar on the vertical axis represents the total discharge, broken up into contributions of water drawn from each of the storage volumes.

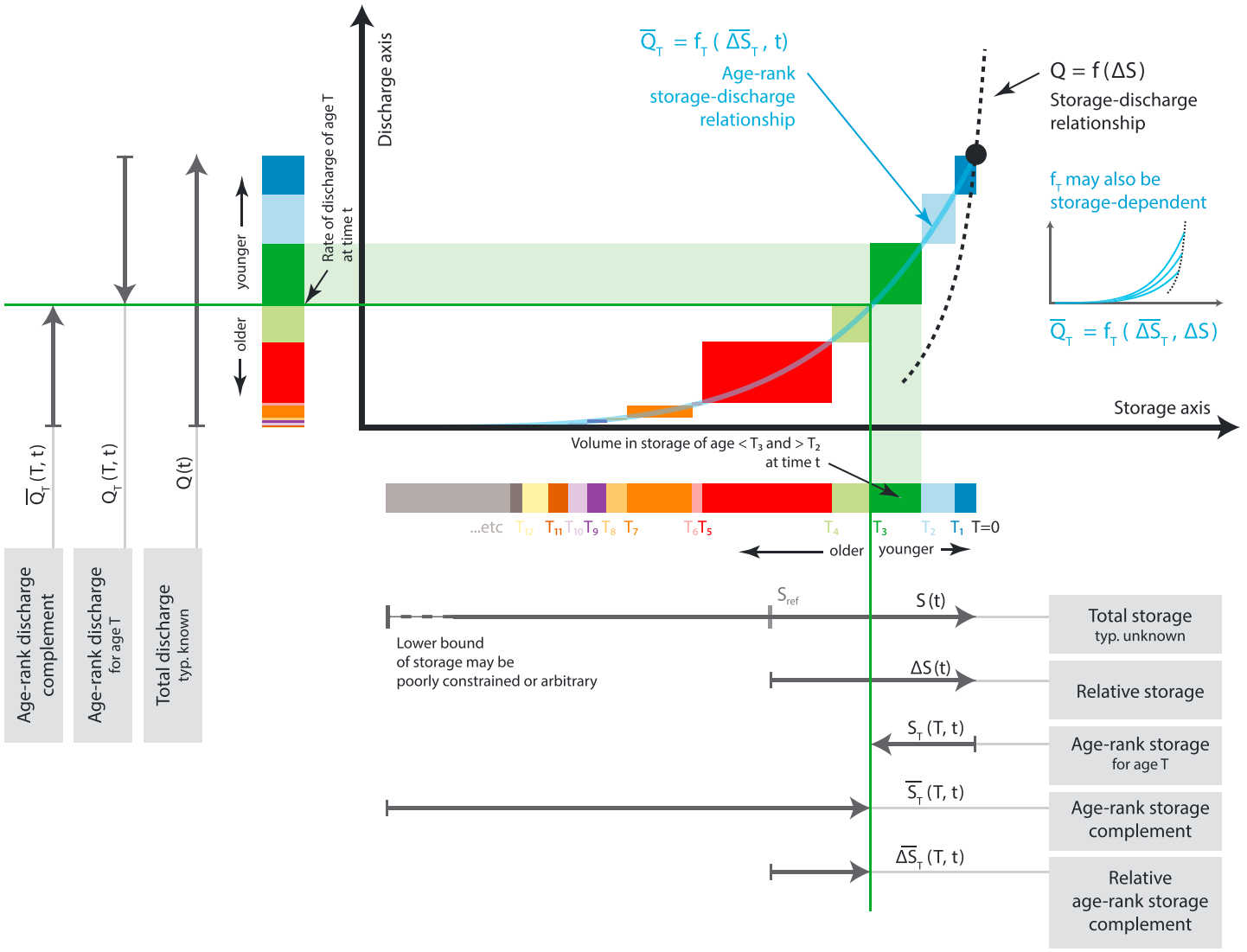

Figure 2. The age-ranked storage-discharge relation $\overline{Q_T} = f_T(\Delta\overline{S_T}, t)$ (the blue curve in the plot above) maps volumes of water of different ages (age-ranked storage—the colored bar sections on horizontal axis) onto rates of discharge of water of different ages (age-ranked discharge—colored bar sections on vertical axis). Note that each color represents a volume of water of a different age. If these stores were associated with time steps or individual storm events, the ages T_1, T_2, and so forth are associated with the start of the time step or event that introduced that water to the system. Note that f_T does not depend on the ages T but only on age rank in storage S_T. At the right hand end of the curve is the total storage S and total discharge Q (black dot). Because absolute storage may not be known, storage is quantified as ΔS relative to some reference state S_{ref}. Both age-ranked storage and age-ranked discharge can be measured from oldest to youngest as $\Delta\overline{S_T}$ and $\overline{Q_T}$ (left to right, bottom to top, respectively, along the colored bars) or vice versa as S_T and Q_T. The total storage and discharge may follow a 1-to-1 storage-discharge relation f (dotted line), or it may be some complex hysteretic relationship. As storage and discharge change, the f_T curve must change also in a way that may, or may not, be uniquely determined by the storage state ΔS (inset plot).

The blue curve f_T describes the relationship between the intervals of age-ranked storage and their corresponding intervals of age-ranked discharge, as the green interval example illustrates. The green interval of age-ranked discharge on the vertical axis is the absolute rate water that is released as discharge from the green interval of age-ranked storage on the horizontal axis. The slope of f_T at a given age rank storage $\Delta\overline{S_T}$ determines the rate water of that age rank is released. Water is released from storage at greater rates from steeper intervals and not at all from flat intervals.

The cumulative release of water from each interval gives the total discharge, so that when $\Delta\overline{S_T} = \Delta S$, we have $\overline{Q_T} = Q$, and so $f_T(\Delta S, t) = Q(t)$. This means that the upper end points of the age-ranked storage-discharge relation (the large black dot in Figure 2) are pinned to the time-varying relationship between storage and discharge. If a functional relationship between storage and discharge (e.g., the dotted black line in Figure 2)

can be said to exist for a given system (in the sense of being a good approximation of the system dynamics over time), then the upper end of f_T will be pinned to it.

However, despite its similarity to a storage-discharge relation (2), the age-ranked storage-discharge relation f_T is fundamentally different: It is a 1-to-1 function defined at a moment in time. That means it is possible to plot the f_T function whether or not a useful storage-discharge relationship $Q = f(\Delta S)$ exists. The f_T function is defined whenever it is possible to define a TTD and SAS function.

2.5. Storage-Dependent Transport and the Inverse Storage Effect

Despite this theoretical distinction, there is evidence to suggest that f and f_T are in fact linked. The SAS function Ω can in principle vary in time and has been observed to do so in a way that is related to storage in experimental systems where tracer data can be used to infer its shape directly (Kim et al., 2016; Pangle et al., 2017). In a number of applications to real catchments, it has proved useful to parameterize the temporal variability of Ω in terms of the storage state ΔS (Harman, 2015; van der Velde et al., 2014). At the catchment scale, this is fundamentally an empirical observation based on an ad hoc model parameterization. The physical origins of this dependence are not well known. However, there has been a few studies that suggest several mechanisms may be important, including the activation of overland flow, macropore flow, and the rise of the water table into relatively transmissive horizons at high storage (Benettin et al., 2017; van der Velde et al., 2012, 2014).

If Ω and f can be written as a function of ΔS rather than t, then of course we can write f_T the same way. The rate water is released from the volume $\Delta\overline{S_T}$ (representing water older than some age T) and is then determined by the relationship:

$$\overline{Q_T} = f_T(\Delta\overline{S_T}, \Delta S), \tag{13}$$

which is to say

$$f_T(\Delta\overline{S_T}, \Delta S) = f(\Delta S)\left(1 - \Omega(\Delta S - \Delta\overline{S_T}, \Delta S)\right). \tag{14}$$

Since $Q = f_T(\Delta S, t)$ (as described above), it must also be the case that $f(\Delta S) = f_T(\Delta S, \Delta S)$ for all ΔS. This means that when f exists, $f_T(\Delta\overline{S_T}, \Delta S)$ is a family of curves that intersect f at a unique point determined by ΔS. This places a constraint on the parameterization of f_T that can be exploited to automatically tie it to ΔS (this will be demonstrated in section 4).

3. The Turnover of Old Water in Storage

So what is the advantage of examining f_T, given that it is simply the product of Q and Ω (rotated and translated by ΔS)? The advantage is that f_T clarifies how changes in both Ω and Q arise from something arguably more fundamental: changes in the release rate of water of different ages from storage.

To be clear, f_T does not introduce new assumptions not already present in Q and Ω. Instead (I would argue), it provides a different way of looking at these quantities. It emphasizes the fact that a change in total discharge may arise from a change in the rate water that is being released from some flow paths, while others perhaps remain unchanged or even change in the opposite direction. In other words, it shows how the potential energy of the system is expended through discharge (at a rate related to the celerity) as a function of the age of the water being released (which is related to the average velocity along the flow path traveled by a parcel of water).

Consequently, the question asked in section 1—how does the turnover of older water change in time?—can be immediately answered by considering changes in the f_T function. It is simply determined by whether the value of f_T at a given $\Delta\overline{S_T}$ increases, stays the same, or decreases. Thus, the f_T presents a different perspective on the hydrologic processes than Ω or Q do alone. The Ω form shows us how the age composition of discharge changes under high flows and low flows, but it does so in a relative sense and obscures the absolute changes.

The Ω and f_T functions suggest subtly different perspectives on the nature of causality. Ω suggests that the changes in age composition are merely occurring at the same time as changes in discharge. In contrast, f_T highlights the fact that the cumulative changes in the rates water of different age ranks are being released from storage *determine* the aggregate change in discharge. When the discharge changes, the f_T function

reveals how that change was driven by an increase or decrease in the release rate across the age-ranked storage.

The f_T function is expressed in terms of $\overline{Q_T}$ and $\Delta\overline{S_T}$ rather than Q_T and S_T to avoid the issue mentioned above: The addition of new water immediately changes the value of S_T associated with a particular parcel of water and so modifies the relationship between S_T and Q_T, even if Q_T is unchanged. On the other hand, the addition of new water that bypasses or never modifies the discharge of older water in the system simply extends f_T to a larger storage (representing the additional volume) and discharge (if any of the additional storage is released immediately). Thus, an invariant physical reality (the rate of old water release unperturbed by the addition of new water) maps to an invariant mathematical structure (the value of f_T at a given $\Delta\overline{S_T}$ unperturbed by a change in ΔS).

These ideas can be made more precise by considering the derivatives of f_T with respect to $\Delta\overline{S_T}$ and ΔS. These each have a meaning that aids in the interpretation of the function. Those meanings are discussed below.

3.1. $\partial\overline{Q_T}/\partial\Delta\overline{S_T}$: Age-Ranked Storage Release Rates

Regardless of whether f_T is assumed to be a function of ΔS, we can take the derivative of $\overline{Q_T}$ with respect to $\Delta\overline{S_T}$. This gives a quantity q_T with the dimensions of a rate [T^{-1}]:

$$q_T = \frac{\partial\overline{Q_T}}{\partial\Delta\overline{S_T}} = \frac{\partial f_T}{\partial\Delta\overline{S_T}}, \tag{15}$$

which is also equal to Q times the unnormalized probability density function of the SAS function ω. This quantity can be usefully (and accurately) interpreted as the rate that water with a given age rank in storage is partitioned to discharge, rather than remain in storage and get older (i.e., it is the volumetric removal rate per volume of storage). It is partially related to the "velocity" of water moving through the lumped system, since the age of water at exit is related to its velocity through the system and the travel distance.

3.2. $\partial\overline{Q_T}/\partial\Delta S$: Age-Ranked Discharge Sensitivity Function

In the special case where Q and $\overline{Q_T}$ are assumed to be a function of ΔS, we can take the derivative of $\overline{Q_T}$ with respect to ΔS. This gives a quantity that is closely related to the catchment sensitivity function $g(Q)$ defined by Kirchner (2009). In a similar way, the derivative of f_T with respect to ΔS is a function that captures the sensitivity of age-ranked discharge to changes in total storage:

$$\frac{\partial\overline{Q_T}}{\partial\Delta S} = \frac{\partial f_T}{\partial\Delta S} = f'_T(\Delta\overline{S_T}, \Delta S), \tag{16}$$

which also has the dimensions of [T^{-1}]. Note that f'_T is defined for a fixed $\Delta\overline{S_T}$, not a fixed T. That is, it is the sensitivity of the rate water is discharged from the oldest $\Delta\overline{S_T}$ volume, not the sensitivity of the rate water is discharged that is older than some age T.

We can also, for the same reasons as Kirchner (2009) laid out, express the resulting function in terms of discharge, rather than storage, and in terms of $\overline{Q_T}$ rather than $\Delta\overline{S_T}$ if f_T is invertible to give $\Delta\overline{S_T} = f_T^{-1}(\overline{Q_T}, f^{-1}(Q))$, so we could define $g_T(\overline{Q_T}, Q) = f'_T(f_T^{-1}(\overline{Q_T}, f^{-1}(Q)), f^{-1}(Q))$. The f_T function may not be invertible however, particularly if some range of young water does not produce discharge, but older water does—this produces a horizontal section of f_T which prevents inversion for $\Delta\overline{S_T}$. Moreover, it is more meaningful to consider g_T for a fixed $\Delta\overline{S_T}$ than for a fixed $\overline{Q_T}$. Therefore, we define

$$g_T(\Delta\overline{S_T}, Q) = f'_T(\Delta\overline{S_T}, f^{-1}(Q)) \tag{17}$$

as the age-ranked discharge sensitivity function, where f'_T is the derivative of (13) with respect to ΔS. If $g(Q)$ can be thought of as capturing the celerity of a system by quantifying the rate that a perturbation in potential energy decays through the release of storage to discharge, the $g_T(\Delta\overline{S_T}, Q)$ function extends this by quantifying how that release is distributed across storage of different ages. To the extent that age and velocity are related, the function therefore represents the interconnection of the celerity and velocity.

3.3. $\partial q_T/\partial\Delta S$ and the Old Water Measurement Problem

One might ask why not take the next logical step and consider the quantity:

$$\frac{\partial^2\overline{Q_T}}{\partial\Delta S\partial\Delta\overline{S_T}} = \frac{\partial qT}{\partial\Delta S}. \tag{18}$$

This quantity might be seen as a synthesis of both the celerity and velocity of water through the system. It is (in the sense alluded to above) the rate that a perturbation in *total* storage is dissipated by a change in the release of a *particular age rank* in storage.

For all its attractiveness as a theoretical construct, this quantity is likely laden with uncertainty. As a second derivative, it may be highly sensitive to properties of the chosen functional form for f_T that are absent or different in other reasonable choices. It is also likely that for storage older than some threshold, the value of q_T is less constrained by passive tracer data (e.g., weekly streamflow and precipitation stable water isotopes) than the value of $\overline{Q_T}$ is. This is because of limitations on the ability of tracers to reveal old-age structure. Streamflow isotopes variability is small and typically can be partially explained by some contribution of the long-term mean isotope composition (Kirchner, 2016). Consequently, it cannot provide decisive information about the relative contribution of, say, 2-year-old versus 2-and-a-half-year-old water but *might* say something about the contribution of water older than 2 years. Similar issues exist for active tracer injection tests, which have difficulty "seeing" the age structure of old water.

These structural and parameter uncertainty issues may be tempered somewhat if instead of attempting to quantify (18) for a particular age rank, we instead choose some subset range of age ranks whose response to hydrologic variability we are interested in

$$\frac{\left.\frac{\partial \overline{Q_T}}{\partial \Delta S}\right|_{\Delta \overline{S_{T2}}} - \left.\frac{\partial \overline{Q_T}}{\partial \Delta S}\right|_{\Delta \overline{S_{T1}}}}{\Delta \overline{S_{T2}} - \Delta \overline{S_{T1}}} \approx \frac{\partial q_T}{\partial \Delta S}, \tag{19}$$

where $[\Delta \overline{S_{T1}}, \Delta \overline{S_{T2}}]$ represents some range in age ranks that is well-characterized by available tracer data.

3.4. Old Water Acceleration, Steadiness, and Suppression

Earlier, we discussed the question of whether old water release increases or decreases when total discharge changes. Put more generally, we can ask how does the function f_T vary in relation to Q (or f, if it exists), and what does this tell us about a hydrologic system?

Since f_T is related to the product of discharge and Ω at a given $\Delta \overline{S_T}$, it can vary in two ways: due to changes in discharge Q (perhaps as determined by f) or due to changes in the shape of Ω. Kim et al. (2016) referred to these as external and internal variability, respectively, as both affect the variability of transit times through the system. External variability modifies that the rate storage is turning over, such that an increase in flow will tend to make storage and discharge younger even when there is no change in the flow pathways through the system. Internal variability implies that the relative contributions of faster and slower flow paths have changed in some disproportionate way, producing a change in the SAS function. Kim et al. (2016) showed that pure external variability can occur in a system in which flow paths and storage vary little when flow through the system changes (as might be case in a confined aquifer or other pressurized hydraulic system at low Reynolds number). They also showed that an increase in discharge in such a system is associated with increases in the turnover rate of all age ranks, and so the SAS function Ω is invariant. (Furthermore, the TTD becomes invariant when expressed in flow-corrected time, as per Rodhe et al. (1996), assuming there is only one flux out of the system).

However, here we are interested in the more general case where discharge, storage, and Ω may all be changing. It would be useful to say something more nuanced about how different age ranks in storage contribute to hydrologic variability.

Let us define a metric characterizing how the discharge of the older part of storage changes relative to changes in total discharge. For a given "older part" of volume $\Delta \overline{S_T}$ at a moment in time t, we define γ as the relative change in $\overline{Q_T}$ per relative change in Q. That is, given a small interval of time δt, let $\delta Q = Q(t+\delta t) - Q(t)$ and $\delta \overline{Q_T} = f_T(\Delta \overline{S_T}, t+\delta t) - f_T(\Delta \overline{S_T}, t)$ and then define $\gamma(\Delta \overline{S_T}, Q)$, which we will call the *old water discharge sensitivity*, as

$$\gamma(\Delta \overline{S_T}, t) = \frac{\delta \overline{Q_T}}{\overline{Q_T}} \Big/ \frac{\delta Q}{Q}. \tag{20}$$

If Ω and storage ΔS are constant, so that (following Kim et al.'s, 2016, definition) all variability is *external* variability, we would expect that some small proportional increment in discharge δQ would be associated

with a proportional increment in age-ranked discharge $\delta\overline{Q_T}$: $\delta\overline{Q_T}/\overline{Q_T} = \delta Q/Q$, so $\gamma = 1$ for all $\Delta\overline{S_T}$. That is, the percent change in each age-ranked discharge matches the overall percent change in discharge.

Further consideration of different possible values of γ suggests a framework for classifying different types of hydrologic behavior:

Old water acceleration when $\gamma > 0$: old water discharge $\overline{Q_T}$ from the volume defined by $\Delta\overline{S_T}$ is increasing/decreasing as total discharge Q increases/decreases;

Old water proportional acceleration when $\gamma \approx 1$: rate of increase/decrease of $\overline{Q_T}$ is proportional (relative to the magnitude) to that of Q;

Old water hyper-acceleration when $\gamma > 1$ rate of increase/decrease of $\overline{Q_T}$ is greater (relative to the magnitude) than that of Q;

Old water steadiness when $\gamma \approx 0$: old water discharge is not changing, so increases/decreases in discharge must be accommodated by increasing/decreasing the turnover of younger water (i.e., only $Q - \overline{Q_T}$ changes); and

Old water suppression when $\gamma < 0$: the increase/decrease in total discharge is associated with a *decrease/increase* in the release of old water.

The value of γ may of course be different for a given $\overline{Q_T}$ at different Q (assuming $Q > \overline{Q_T}$) and for a given Q at different $\overline{Q_T}$.

In previous work, Harman (2015) defined the inverse storage effect as the tendency of catchments to preferentially release younger water under wet conditions. In the framework developed above, this corresponds to $\gamma < 1$. Note that the observation of an inverse storage effect does not imply that there is old water suppression or acceleration. Both are possible, and more detailed analysis of f_T is required to determine which is the case.

3.5. Relationship Between Old Water Sensitivity γ, SAS Functions Ω, and Catchment Sensitivity g

We can express γ in terms of the SAS function $\Omega(S_T, t)$ directly by taking the time derivative of equations (11) and (12). Note that since Ω is expressed in terms of S_T rather than $\Delta\overline{S_T}$, we are obliged to account for the relative storage ΔS that relates these two quantities (by equation (9)) and its increment in time δS. Taking the limit of small δt, we get

$$\gamma(\Delta\overline{S_T}, t) = 1 - \frac{\frac{\partial\Omega}{\partial t} + \frac{\mathrm{d}\Delta S}{\mathrm{d}t}\frac{\partial\Omega}{\partial S_T}}{\frac{\mathrm{d}Q}{\mathrm{d}t}\frac{1-\Omega}{Q(t)}} \tag{21}$$

If Q and Ω are assumed to be functions of ΔS (as in equation (13)), it is also possible to express γ in terms of the sensitivity functions g and g_T, since we can say $\delta Q = g(Q)\delta S$ and $\delta\overline{Q_T} = g_T(\Delta\overline{S_T}, Q)\ \delta S$. Then $\gamma(\Delta\overline{S_T}, Q)$ is simply

$$\gamma(\Delta\overline{S_T}, Q) = \frac{g_T(\Delta\overline{S_T}, Q)}{\overline{Q_T}} \Big/ \frac{g(Q)}{Q}. \tag{22}$$

Or alternatively in terms of $\Omega(S_T, \Delta S)$

$$\gamma(\Delta\overline{S_T}, Q) = 1 - \frac{\frac{\partial\Omega}{\partial\Delta S} + \frac{\partial\Omega}{\partial S_T}}{g(Q)\frac{1-\Omega}{Q}}, \tag{23}$$

where Ω and its partial derivatives are evaluated at $S_T = \Delta S - \Delta\overline{S_T}$.

From the expressions above, we can see that indeed $\gamma = 1$ if Ω and ΔS are invariant in time, as expected given Kim et al.'s (2016) definitions of internal and external variability. However, a system with variable storage can also have $\gamma = 1$ if Ω is variable such that

$$\frac{\partial\Omega}{\partial t} = -\frac{\mathrm{d}\Delta S}{\mathrm{d}t}\frac{\partial\Omega}{\partial S_T}. \tag{24}$$

For a system to have $\gamma = 0$ (old water steadiness), then $g_T(\Delta\overline{S_T}, Q) = 0$, and the shape of the SAS function must satisfy

$$\frac{\partial \Omega}{\partial t} = \frac{\mathrm{d}Q}{\mathrm{d}t}\frac{1-\Omega}{Q(t)} - \frac{\mathrm{d}\Delta S}{\mathrm{d}t}\frac{\partial \Omega}{\partial S_T}, \tag{25}$$

or

$$\frac{\partial \Omega}{\partial \Delta S} = g(Q)\frac{1-\Omega}{Q} - \frac{\partial \Omega}{\partial S_T}. \tag{26}$$

This is due to the fact that the Ω function describes the SAS of water in terms of S_T (which progresses from the youngest to the oldest) so that the addition of new water changes the value of S_T associated with a particular parcel of older water. Equations (25) and (24) describes how Ω would need to change to compensate if the release rate of that older water is to remain invariant.

4. Power Law Age-Ranked Storage-Discharge Relations: A Simple Theoretical Case With Constant γ

It can also be useful to choose some parsimonious functional form (i.e., with few parameters) with interesting features and consider what we can learn from its (in)ability to capture the essential behavior in a top-down manner (Farmer et al., 2003; Jothityangkoon et al., 2001). Here we consider the unified elementary case of a power law model for both the storage-discharge *and* the age-ranked storage-discharge relationship. The resulting model has the interesting feature of a constant value of γ. This highlights a potential advantage of considering how Ω and Q combine to produce f_T—doing so allows us to address the acceleration/suppression dynamics directly and perhaps even parameterize the model in terms of these dynamics.

Plots of $\log(-\mathrm{d}Q/\mathrm{d}t)$ versus $\log Q$ sometimes appear (with some considerable scatter) to be approximately linear, with a slope that is conventionally termed b (Brutsaert & Nieber, 1977). There are several different models that can reproduce this behavior (Harman et al., 2009; Rupp & Selker, 2006), but a simple one is a power law storage-discharge relationship of the form $f(\Delta S) = m\Delta S^n$. In that case it can be easily shown that n is related to b as $n = 1/(2-b)$. Kirchner (2009) showed that a dimensionally consistent way of expressing m can be obtained by breaking it into three parts, so that $m = Q_{\mathrm{ref}}((2-b)/s)^n$. Note that by replacing one variable with two purely for the purpose of dimensional consistency, we introduce a degree of freedom. Consequently, we can set the value of one of Q_{ref} or s to be arbitrary, though the choice will influence the value of the other needed to produce the "correct" m (see ; Dralle et al., 2015, for a discussion of the surprising consequences of this arbitrariness). Here we will take Q_{ref} to be the arbitrary scaling factor. Q_{ref} and s are assumed to be positive with units of discharge and storage, respectively. Thus, the storage-discharge relation can be expressed as

$$f(\Delta S) = Q_{\mathrm{ref}}\left(\frac{(2-b)\Delta S}{s}\right)^{\frac{1}{2-b}}. \tag{27}$$

This function can also be inverted and expressed as

$$\frac{S - S_{\mathrm{ref}}}{s(2-b)} = \left(\frac{Q}{Q_{\mathrm{ref}}}\right)^{2-b}. \tag{28}$$

The power law storage-discharge relationship can be thought of as having three parameters: b (discussed below), a scale parameter (which is m but which here is determined by s), and the shift S_{ref} that determines the value of S at which ΔS goes to zero. Even though we do not typically know S_{ref}, we can implicitly modify its value by shifting ΔS by a constant and so change the state of storage that corresponds with $\Delta S = 0$. Since the power law above will either produce $Q = 0$ or $Q = \infty$ when $\Delta S = 0$, the value of S_{ref} is an important control, despite its absolute value being unknowable.

As discussed by Kirchner (2009), when $0 < b < 2$, the value of $\Delta S = S - S_{\mathrm{ref}}$ must be positive. S_{ref} is the storage (or rather, the maximum storage) at which $Q = 0$. On the other hand, when $b > 2$, this model only

produces positive values for discharges that increase with storage if we assume ΔS is negative, so $S < S_{\text{ref}}$. In this case discharge becomes asymptotically large as storage approaches S_{ref} (i.e., $\Delta S \to 0$ from below). Consequently, $|\Delta S|$ is the current deficit of storage below this upper limit.

In order to better understand the relationship between total and age-ranked storage-discharge relations, it may be useful to adopt a similar (and similarly simple) mathematical form for f_T as for f. Let us assume that the age-ranked storage-discharge relationship also follows a power law:

$$f_T(\Delta\overline{S_T}, \Delta S) = Q_{\text{ref}}\left(\frac{(2-b_T)(\Delta\overline{S_T} - \Delta S_c)}{s_T}\right)^{\frac{1}{2-b_T}}. \tag{29}$$

As with (27), this expression has three parameters: an exponent b_T, a scale parameter determined by s_T, and a shift S_c. By expressing this shift relative to S_{ref} (as $\Delta S_c = S_c - S_{\text{ref}}$), we can associate this shift parameter with a particular value of $\Delta\overline{S_T}$. The meaning of ΔS_c depends on the exponent b_T, as discussed below. The arbitrary discharge scale Q_{ref} can be taken to be the same in both expressions with no loss of generality. However, we must satisfy the requirement that $f_T(\Delta S, \Delta S) = f(\Delta S)$. This reduces the degrees of freedom in equation (29) by one parameter. Setting (27) and (29) equal to each other with $\Delta\overline{S_T} \to \Delta S$ and solving for s_T gives

$$s_T = \left(2 - b_T\right)\left(\Delta S - \Delta S_c\right)\left(\frac{(2-b)\Delta S}{s}\right)^{-\frac{2-b_T}{2-b}}. \tag{30}$$

Thus, one way to satisfy the requirement would be to determine s_T from the equation above, rather than allowing it to be a free parameter (to be determined by fitting to data). An alternative would be to determine either ΔS_c or b_T by rearranging the equation above. For ΔS_c, this gives

$$\Delta S_c = \frac{s_T\left(-\frac{(b-2)\Delta S}{s}\right)^{\frac{b_T-2}{b-2}}}{b_T - 2} + \Delta S, \tag{31}$$

and for b_T, this gives

$$b_T = 2 + \frac{(2-b)W\left(-\frac{s_T \log\left(\frac{(2-b)\Delta S}{s}\right)}{(2-b)(\Delta S - \Delta S_c)}\right)}{\log\left(\frac{(2-b)\Delta S}{s}\right)}, \tag{32}$$

where $W(\cdot)$ is the Lambert W (or Product Log) function (Abramowitz & Stegun, 1964). Through these equations, the value of one of s_T, ΔS_c, or b_T becomes dependent on the storage state ΔS.

Here we have chosen to keep b_T and ΔS_c as constant free parameters and allow s_T to be determined by the constraint. In this case the value of γ becomes independent of $\Delta\overline{S_T}$ (as discussed below)—this is not true if ΔS_c or b_T are used instead. This is similar to the choice made in Harman (2015) to allow the scale parameter of the gamma distribution to vary while keeping the shape parameter constant.

Thus, the combined model for f and f_T has four free parameters (b, b_T, s, and ΔS_c) and an arbitrary reference discharge Q_{ref}.

Substituting the constraint on s_T back into (29) yields the rather elegant relationship:

$$\frac{\overline{Q_T}}{Q} = \frac{f_T(\Delta\overline{S_T}, \Delta S)}{f(\Delta S)} = \left(\frac{\Delta\overline{S_T} - \Delta S_c}{\Delta S - \Delta S_c}\right)^{\frac{1}{2-b_T}}. \tag{33}$$

In this equation we can start to see the consequences of assuming these two simple power law relationships for f and f_T. Figure 3 illustrates this with examples.

If $0 < b_T < 2$, the critical age-ranked storage ΔS_c represents the lower bound of the storage that is turning over and contributing water to discharge. It is the value of $\Delta\overline{S_T}$ at which $\overline{Q_T} = 0$. Therefore, ΔS_c must always be less than the storage state ΔS. The storage volume $-\Delta S_c$ effectively represents a "dead store" that cannot be drained even in very long streamflow recessions, but it does turn over and contribute to streamflow. If

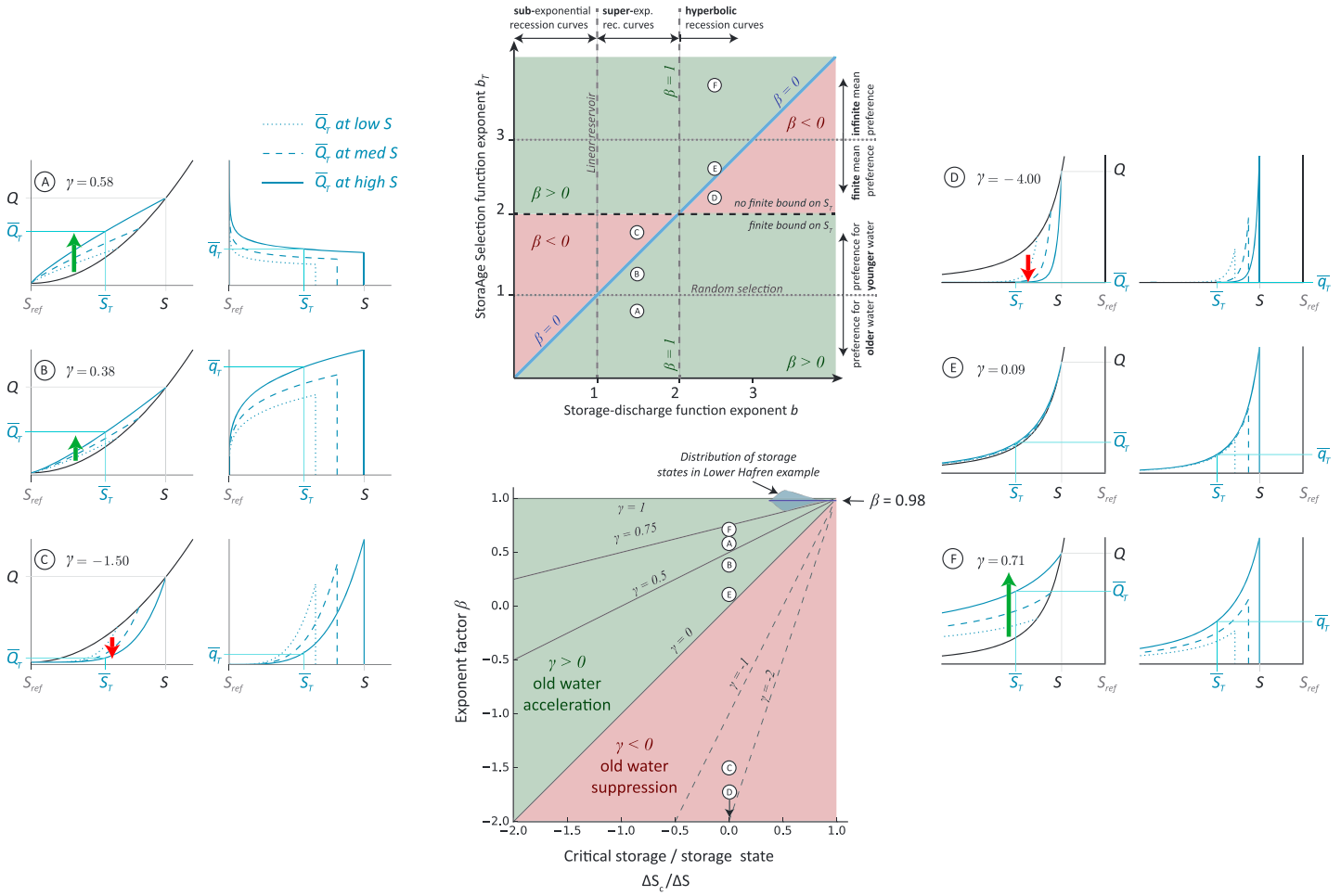

Figure 3. Classification of different types of old water release dynamics for the power law f and f_T case described in section 4. Upper center plot shows the sign of the β (given in equation (37)) for different exponents b and b_T and the way these exponents control the properties of the storage-discharge and age-ranked storage-discharge relation. The lower plot shows how the value of the critical storage parameter ΔS_c and β determine the old water sensitivity γ. On either side, the inset plots show the f (solid black line) and f_T for different storage states (blue lines) corresponding with the combinations of b and b_T on the center plots (with $\Delta S_c = 0$). When $\gamma > 0$, there is old water acceleration (green arrows), and when $\gamma < 0$, there is old water suppression (red arrows). When $\gamma \approx 0$, old water discharge is steady, and additional discharge comes from the release of new water (plot E). The distribution of values of γ for the Lower Hafren is also shown on the lower plot.

$b > 2$, discharge never reaches zero for any ΔS, so as storage declines toward ΔS_c, the slope of $\overline{Q_T}$ becomes steeper and steeper, until only the youngest water remaining in the system is removed as discharge. Beyond that point, $\Delta S < \Delta S_c$, and the model is not valid.

If $b_T > 2$, the volume of water turning over and contributing to discharge is effectively infinite, but older water contributes asymptotically small amounts. In this case ΔS_c represents an upper bound of age-ranked storage at which $\overline{Q_T}$ becomes infinitely steep (i.e., a step function from 0 to Q), so that all discharge is selected from only the very youngest water in the system. Total storage cannot therefore be higher than this (i.e., we require $\Delta S_c > \Delta S$ always). If $0 < b < 2$, the storage below $\Delta \overline{S_T} = 0$ is again a dead store that contributes to discharge but cannot be drained. If $b > 2$, it can be drained (mathematically speaking) down to any level of storage depletion given enough time.

Using the relationship in equation (14), we can obtain the SAS function equivalent for (29)

$$\Omega(S_T, \Delta S) = 1 - \left(1 - \frac{S_T}{\Delta S - \Delta S_c}\right)^{\frac{1}{2-b_T}}, \tag{34}$$

where $\Delta S - \Delta S_c$ takes the role of a scale parameter that varies linearly with storage and goes to zero when $\Delta S = \Delta S_c$. For $-\infty < b_T < 2$, this is a Kumaraswamy distribution on the bounded interval $0 \leq S_T \leq$

$\Delta S - \Delta S_c$. This distribution is similar to the Beta distribution used by van der Velde et al. (2012) and others to parameterize the SAS function. For $b_T > 2$, it is fundamentally a different distribution as the sign of $\Delta S - \Delta S_c$ is negative, and support of the distribution is the entire positive real axis $S_T > 0$. This is actually a Lomax distribution, which is a special case of the generalized Pareto distribution. Either way, the mean of the distribution is given by

$$\mu = \frac{2 - b_T}{3 - b_T} \left(\Delta S - \Delta S_c \right), \tag{35}$$

if $b_T < 3$. For $b_T > 3$, the mean is undefined. If this model were to provide a good fit to real tracer data with $b_T > 3$, we would have to conclude that the tracer data must only be constraining the SAS of a small fraction of the total storage volume and could not constrain the behavior of the larger part.

With some manipulation, we can also obtain an expression for the old water sensitivity function as

$$\gamma = \frac{\beta - (\Delta S_c / \Delta S)}{1 - (\Delta S_c / \Delta S)}, \tag{36}$$

where β is a bounding value of γ given by

$$\beta = \frac{b - b_T}{2 - b_T}. \tag{37}$$

Interestingly, γ is a function of ΔS but is independent of $\Delta \overline{S_T}$—thus, the sensitivity is the same for all age-ranked storage. In the special case that $\Delta S_c = 0$, we have $\gamma = \beta$, and γ is a constant than only depends on b and b_T. The scale parameter s provides a storage scale (in conjunction with the arbitrary Q_{ref}) that will interact with the variability of inputs (J) to control the actual time scale of discharge variability and storage turnover. But in a certain sense, the underlying structure is set by only the two exponents, modified by the storage state if $\Delta S_c \neq 0$.

This allows us to think about a simplified classification of types on the basis of b and b_T and the ratio $\Delta S_c / \Delta S$. Figure 3 shows how β varies for different combinations of b and b_T, and some of the types of behavior that arise. For $b = 1$, the storage-discharge relationship is a familiar linear reservoir, and for $b_T = 1$, the SAS is uniform, as would be expected in a well-mixed tank (Danckwerts, 1953), homogeneous semiconfined aquifer (Haitjema, 1995), or highly dispersive system (Benettin et al., 2013).

Other combinations of b and b_T produce different characteristics of storage age selection, as shown. The green and red domains in the top plot show the combinations of b and b_T for which $\gamma > 0$ (old water acceleration) and $\gamma < 0$ (old water suppression), respectively, for the special case that $\Delta S_c = 0$. The lower plot shows the way γ is modified by the value of ΔS_c. Plots on either side show the age-ranked storage-discharge relation f_T and storage release rate q_T for a variety of combinations of b and b_T, all assuming $\Delta S_c = 0$. These illustrate (A) old water preference, (B) old water acceleration, and (C) old water suppression in a storage with a finite lower bound. Plots (D)–(F) show old water suppression, steadiness, and acceleration (respectively) for a system without a finite lower bound.

The lower plot in Figure 3 shows the values of γ calculated from equation (36) for other values of ΔS_c. These show that for a given value of β, the value of γ declines (moving toward less old water acceleration and more suppression) as ΔS approaches ΔS_c. Note that for $0 < b < 2$, this happens when ΔS is decreasing (since $\Delta S > \Delta S_c$ in that case), but for $b > 2$, it occurs when ΔS is increasing (since $\Delta S < \Delta S_c$).

5. Example Applications

The concepts of the age-ranked storage-discharge relation f_T and old water sensitivity γ can be illustrated using published case studies that have employed SAS functions determined using tracer data. We can use the Ω and f functions obtained in those studies to obtain f_T and its related quantities. In the second example, the power law f_T derived above will also be applied to the original data and the results compared.

5.1. Stream-Hyporheic Flow and Transport, H. J. Andrews, WS01 Reach

Harman et al. (2016) applied the SAS approach to analyze stream tracer injection and recovery along a stream reach in a forest. Over a 28-hr period, salt slugs were introduced at the upstream end of the reach, and breakthrough curves were obtained at upstream and downstream electrical conductivity probes spaced

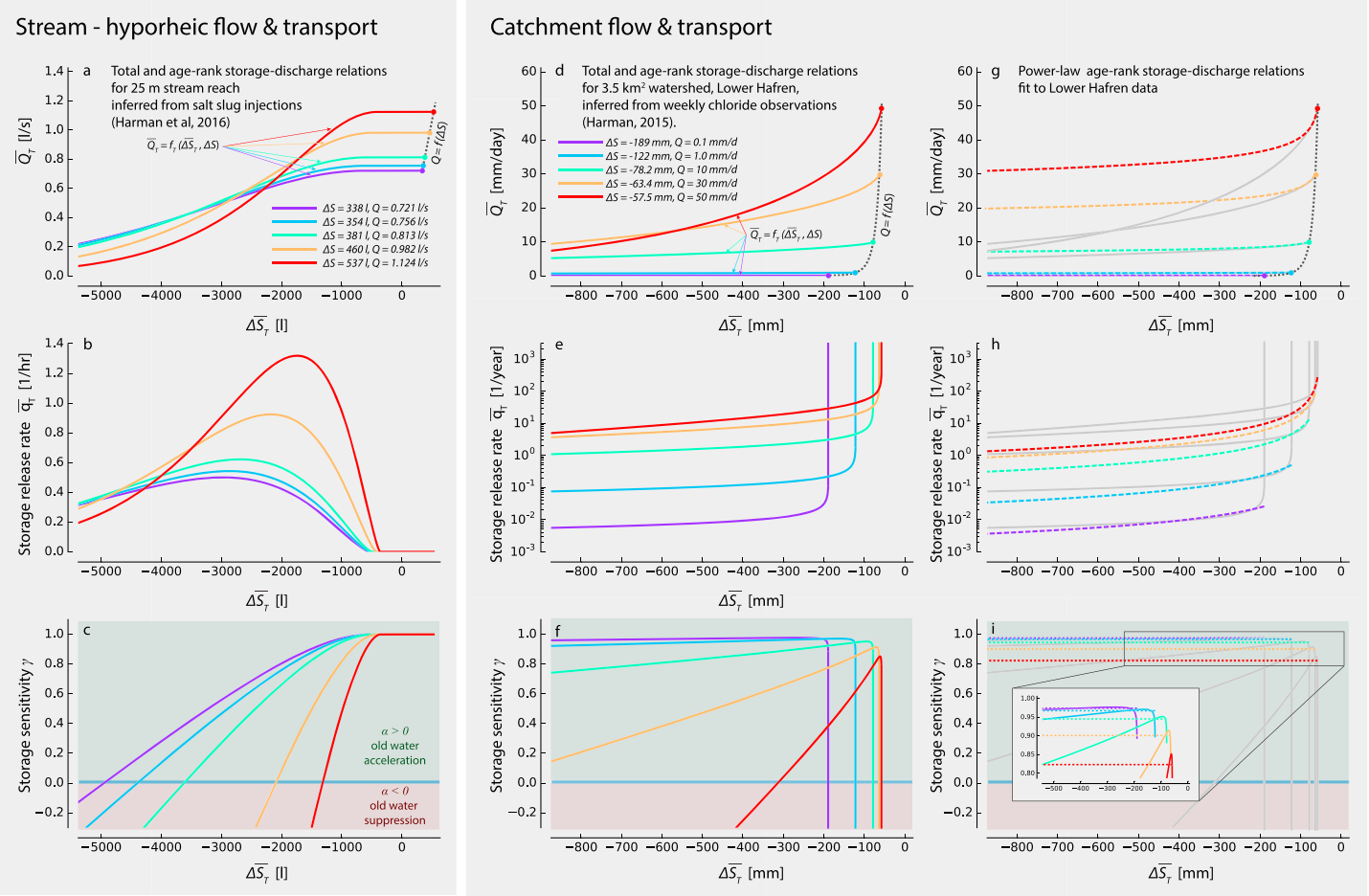

Figure 4. Application of the theory to data from (a–c) an active tracer injection in a short reach reported in Harman et al. (2016) and (d–f) catchment-scale passive tracer data reported in Harman (2015) and (g–i) is a power law f_T fit to the same catchment data. The top row shows age-ranked storage-discharge relations. Each colored solid line represents f_T for a different value of ΔS. Middle row shows the corresponding age-ranked storage release rate q_T, and the bottom row shows the old water sensitivity γ.

25 m apart. Over the study period, discharge varied between 0.74 and 1.2 L/s as part of a diurnal cycle typical of this stream in the late dry season (Wondzell et al., 2009, 2007).

Stream depth observed with pressure transducer varied linearly with discharge at the nearby gauge (Harman et al., 2016) suggesting an approximately linear storage-discharge relationship. Using estimates of effective stream width and length, Harman et al. (2016) obtained a storage-discharge relationship given by $Q = f(\Delta S) = k\Delta S$, where $k = 7.7\ \mathrm{hr}^{-1}$. Here $\Delta S = 0$ represents the relative storage at which discharge is zero. Note that this does not imply that when discharge is zero, storage (even within-channel storage) is also zero. It is merely a reference datum for storage with some useful physical interpretation, and one well outside the range of relative storages inferred from the data. Values of ΔS actually ranged from 336 to 557 L.

The time series of seven breakthrough curves was found to be well approximated by modeling the SAS function Ω as a shifted gamma distribution whose parameters vary with discharge (Harman et al., 2016, table 2, Nash Sutcliffe Efficiency = 97%). Specifically, discharge was assumed to be linearly related to the mean, standard deviation, and shift of the Ω function as $S_\mu = 4{,}279\text{–}4{,}084 \times (Q - 0.870)$, $S_\sigma = 2{,}698\text{–}2{,}431 \times (Q - 0.870)$, and $S_{\min} = 874\text{–}60 \times (Q - 0.870)$ for Q in liters per second and S_μ, S_σ, and $S_{\min}$ in liters. These were then used to obtain the scale parameter β and shape parameter α of the gamma distribution as $\beta = S_\sigma^2/(S_\mu - S_{\min})$ and $\alpha = S_\sigma^2/\beta^2$. The predicted f_T was then obtained from equation (14).

The resulting age-ranked storage-discharge functions f_T (and f) are shown in Figure 4. The SAS modeling suggested that over the 4 hr between each tracer injection, the tracer-labeled water reached an age rank of around $\Delta\overline{S_T} = -5{,}000$ L, so behavior for larger age ranks is not informed by data and is not shown.

The inferred f_T functions suggest there are three ranges of $\Delta\overline{S_T}$ over which $\overline{Q_T}$ behaves in different ways. At the highest values of $\Delta\overline{S_T}$ (representing the youngest water in the system), the f_T function is flat, which indicates that no discharge is drawn from that (approximately 750–950 L) storage. This represents the advective delay along the stream channel (Benettin et al., 2013). Over an intermediate domain of $\Delta\overline{S_T}$ from about −2,500 to −800 L, the value of f_T increases with increasing ΔS. Below that, it stays nearly constant for low ΔS and decreases for high ΔS.

The age-ranked storage release rate (Figure 4) provides a clear picture of how storage turnover changes with age rank. As ΔS and Q increase, the advective storage volume does not change in a consistent way, so $q_T = 0$ over a fairly constant range at the highest $\Delta\overline{S_T}$. Increases in Q are associated with increases in the rate of turnover of the next oldest $\Delta\overline{S_T}$, and peak turnover rates are found at younger and younger $\Delta\overline{S_T}$. The peak turnover rate varies from around $q_T = 0.5$ hr^{-1} at $\Delta\overline{S_T} = -3,000$ L at the lowest flow to $q_T = 1.3$ hr^{-1} at $\Delta\overline{S_T} = -1,740$ L at the highest flow. Storage in the oldest tracer-labeled age-ranked storage does not seem to turn over faster at higher discharge. The apparent decline in turnover rate at the highest discharge is small and may be an artifact of the structure of the chosen functional form for Ω. The more substantial decline in q_T at even lower age ranks below the plotted range is not supported by the data (as discussed in ; Harman et al., 2016). Thus, it seems plausible that the discharge of water drawn from $\Delta\overline{S_T}$ below −4,000 to −3,000 L is in fact invariant with respect to ΔS and Q. Harman et al. (2016) suggested that this relatively constant turnover rate may be driven by the down-valley topographic gradients and not by the in-stream processes, corroborating observations from others studying the same reach (Ward et al., 2016; Ward et al., 2017; Schmadel et al., 2017).

The limitations on the old water mobilization behavior imposed by the choice of a gamma function for Ω are illustrated by the plot of the acceleration factor γ (Figure 4). Here γ was determined by taking the numerical derivative of $\overline{Q_T}$ with respect to $\Delta\overline{S_T}$, as parsimonious analytical solutions could not be found. The figure shows that $\gamma = 1$ in the advective delay storage, reflecting the fact that increases in discharge are always accommodated by increases in the release of water older than that which is in transit along the fastest pathway through the reach. The γ then declines monotonically for lower $\Delta\overline{S_T}$. If the suggestion above is true and old water turnover is actually insensitive to ΔS and Q, then these curves ought to not drop below $\gamma = 0$. However, the chosen functional form does not permit this.

5.2. Catchment Flow and Transport, Lower Hafren Stream

Harman (2015) applied the SAS approach to model chloride transport in the Lower Hafren stream, a 3.5-km^2 catchment in Plynlimon, Wales. The Lower Hafren has a long record of stream gauging and chemistry from weekly precipitation and streamflow samples. TTDs have been examined in this watershed in the past using chloride as an (assumed) conservative tracer, and storage-discharge relations have been analyzed in the larger Severn River (Kirchner, 2009) of which it is a part.

Harman (2015) assumed that the SAS function of discharge was a gamma distribution whose scale parameter S_0 was linearly related to relative storage ΔS, as $S_0 = \lambda(\Delta S - \Delta S_c)$. Thus, in addition to the shape parameter α, the parameters λ and ΔS_c had to be calibrated against the observed stream chloride data. Relative storage was determined by fitting a catchment sensitivity function using the methods of Kirchner (2009) and integrating to obtain ΔS. The value of S_{ref} was set to the mean storage (this only affects the apparent value of ΔS_c). The λ parameter represents the sensitivity of the SAS function to variations in ΔS, and ΔS_c is the storage state at which the scale parameter reaches zero. At that point, the SAS function collapses into a Dirac Delta distribution, and all discharge is drawn from the youngest water in storage. The evapotranspiration SAS function was assumed to be an invariant uniform distribution over the youngest storage S_{ET}. All water in storage at the start of the simulation was assumed to have a fixed concentration $C_{\text{old}} = 7.11$ mg/L, which was the observed flux-weighted mean discharge concentration. Fitted values reported by Harman (2015) are $\lambda = 103$, $\Delta S_c = 48$ mm, $\alpha = 0.69$, and $S_{\text{ET}} = 398$ mm.

Figure 4 shows the storage-discharge relation f and the age-ranked storage-discharge relation f_T for the observed range of daily discharges. The f curve appears relatively steep in this plot compared to f_T, as the observed range of storage ΔS (about 106 mm over 27 years of record) is much smaller than the mean of the SAS function (which varies from day to day with storage but was around 3,300 mm on average). The f_T function is nearly flat at low discharges, suggesting water is drawn from a very large storage. At higher storage, the discharge of older water (lower $\Delta\overline{S_T}$) is greater, but the slope of the f_T function at the right-hand end also increases, indicating that the contributions of younger water are increasing faster. For the highest discharge

(the red line in Figure 4), the contributions of old water appear to have actually decreased, suppressed by the increasing contributions of young water.

This rapid increase in young water contributions with increasing storage and discharge was termed the inverse storage effect by Harman (2015). It can also be clearly seen in the plot of age-ranked storage release rate q_T in Figure 4 (note the log scale). As discharge increases, the rate of storage turnover increases for all values of S_T. However, the increment of q_T is larger for younger storage than it is for older, indicating that the increase in discharge is disproportionately accommodated by an increase in the rate of release of young water.

Despite the inverse storage effect, the old water sensitivity factor is typically $\gamma > 0$ suggesting that old water is generally accelerated at moderately high flows. Only at the highest flows does there appear to be a suppression of old water. However, as with the previous example, it seems this old water suppression may be an artifact of the choice of a gamma distribution for Ω.

5.3. Comparison of Gamma and PowerLaw f_T in Lower Hafren

In the examples above, the chosen functional form for Ω placed constraints on how γ could vary across age ranks. A different functional form, with different constraints on γ, might produce similarly good fits to the data but could imply quite different old water sensitivity for age ranks where the SAS function is poorly constrained by data. This uncertainty about which functional form is the "best" (or even which might be grounded in some sort of physical model) is a kind of "structural uncertainty" (Ajami et al., 2007; Clark et al., 2008).

The constant value of γ in the power law form of f_T derived in section 4 is a useful counterpoint to the gamma distribution considered above. The power law model was fit to Lower Hafren data (1983–2008) using the same approach as described in Harman (2015). Best-fit parameters were calibrated by minimizing root mean square error (RMSE) of predicted chloride concentration for a 10-year period (1989–1998), and performance was checked against a 10-year validation period (1999–2008). A 7-year spin-up period was allowed. The fitted parameters are $b = 2.2$, $s = 12.7$ mm (with $Q_{\text{ref}} = 1$ mm/hr), $b_T = 12.2$, and $\Delta S_c = -53$ mm. The evapotranspiration SAS function from Harman (2015) was used (uniform distribution over the youngest storage $S_{\text{ET}} = 398$ mm).

This alternative functional form had a comparable fit to the observed data (gamma distribution RMSE: 0.91-mg/L calibration and 0.98-mg/L validation and power law RMSE: 0.90-mg/L calibration and 0.95-mg/L validation). However, the power law model makes very different predictions about the mobilization of old water.

Figure 4 shows the power law age-ranked storage-discharge relations. They closely agree with the gamma distribution at low storage and discharge and for the youngest age-ranked storage. But where the gamma distribution suggested that old water is not mobilized as strongly at high flows and is in fact suppressed at the highest flows, the power law predicts a consistent mobilization of old water into discharge. It essentially predicts that the volume of old water that is being mobilized is much larger (and the rate of turnover q_T at a given $\overline{S_T}$ is smaller, as seen in Figure 4).

In fact, not just larger but infinite. Since $b_T > 3$, the mean of the SAS distribution is infinite, which is not physically possible. Despite being physically impossible, the power law model reproduces the chloride behavior as well as the gamma distribution.

Why is this? A clue can be seen in comparing the plot of γ for the gamma and power law approaches shown in Figure 4 and highlighted in the inset plot. The two functions give similar degrees of old water mobilization for a narrow range of age-ranked storage, and that range gets narrower at high flows. This suggests that the model fit (as measured by RMSE at least) is insensitive to the model predictions of old water mobilization beyond some threshold $\Delta\overline{S_T}$. This is in accordance with other studies suggesting that the chloride tracer data does not constrain the old water contributions in this watershed (Kirchner et al., 2000).

6. Discussion and Conclusion

This paper has laid out the basic connections between storage-discharge relations and SAS functions and suggested the age-rank storage-discharge relation as way to understand them. This is a curve $\overline{Q_T} = f_T(\Delta\overline{S_T}, t)$

that maps age rank in storage onto age rank in discharge, such that the end point of the curve represents the total storage and total discharge at a point in time. The trajectory of this end point represents the time-variable (possibly hysteretic) relationship between storage and discharge. Where the relationship has limited hysteresis, a storage-discharge relation $f(\Delta S)$ can be seen as the upper boundary of a family of age-ranked storage-discharge relationships $f_T(\Delta\overline{S_T}, \Delta S)$.

The concepts of celerity and velocity have also been discussed in the sense proposed by McDonnell and Beven (2014). The catchment sensitivity function $g(Q)$ has been discussed as a means to approximately quantify celerity and the TTD as a means to quantify velocity when considering lumped systems. Quantities obtained from the two partial derivatives of the f_T curve can be seen as representing the way transport variability in the system is determined by (respectively) the velocity and celerity.

I have argued that f_T could serve to extract a clearer picture of catchment processes from tracer data than consideration of Ω alone. This is not to say that we should dispense with consideration of Ω. Rather, there is information in f_T useful to the investigation and modeling of runoff generation and transport that cannot be discerned when Q and Ω are considered separately. Figure 2 visualizes the relationship between age-ranked storage and discharge (expressed in terms of the complementary quantities $\Delta\overline{S_T}$ and $\overline{Q_T}$). It is likely useful even if discharge relation (and its age-ranked extension) is not a unique function of storage ΔS, as it is defined for each moment in time. This can be used to examine the effects of old water suppression and acceleration even in the case of complex hysteretic relationships.

6.1. Old Water Suppression and Acceleration: Artifact or Reality?

The phenomena of old water suppression and acceleration have been described and illustrated using data. These concepts may be useful for understanding the dynamics of old and young water in the landscape. There has been some progress using SAS functions to understand the influence of global change on young water fractions (e.g., ; Wilusz et al., 2017), but a deeper understanding of the effects of changes in recharge on old water storage and release is needed to make meaningful projections about the impact of global change. The oldest water fractions are especially relevant to issues of drought resilience (e.g., ; McGuire et al., 2002) and nutrient lag times (Van Meter & Basu, 2015).

It is possible to conceive of physical mechanisms that might generate such a suppression. For example, observations of the groundwater table at the toe of hillslopes in gentle terrain suggest that during storm events, the higher rates of recharge there (relative to further upslope where the water table is deeper) generate adverse hydraulic gradients away from the stream (Zimmer & McGlynn, 2017). The adverse slope could conceivably reduce the absolute (not just proportional) rate old water is delivered to the stream during high flows, thus creating a negative value of γ. More investigation is needed to test this hypothesis though.

Unfortunately, as has been demonstrated in the catchment example presented here, catchment passive tracer data such as conservative ionic and isotopic tracers from precipitation may be insufficient to determine whether old water acceleration or suppression is occurring. The gamma and power law models provided similarly good fits to the data but made radically different (though similarly unrealistic) assertions about the mobility of old water in the catchment.

The application of the framework in the examples revealed that the gamma SAS function used by Harman et al. (2016) and Harman (2015) embeds some potentially unrealistic structure. The functional form requires old water suppression for a portion of the storage, and that portion gets larger at high flows. Although I have suggested this phenomenon could potentially be real, we cannot draw any conclusions since it is not possible for the gamma SAS function to *not* produce this behavior.

Furthermore, the power law model does not produce old water suppression in this case. However, it is not possible for this functional form to produce old water suppression while also capturing the mobilization of younger water needed to reproduce the data. Consequently, the SAS function implied by this functional form also shows some potentially unrealistic behavior of an opposite character to the gamma distribution. The value of γ is constant for all $\Delta\overline{S_T}$ implying old water acceleration throughout the storage. The degree of acceleration is so large that it must be drawn from a very large storage in order to be sustained. The value of $b_T = 12.2$ implies that even at the highest flows, less than half the water is drawn from the youngest 4 m of storage—the rest is drawn from an even larger volume. It seems unrealistic to imagine that the majority of peak discharges is released from such a large volume.

The indeterminacy regarding the true behavior of the old water can be understood as a consequence of the ability (or lack thereof) of the available data to constrain the parameters of the given functional form and to assess the goodness of fit of the resulting predictions. With additional data or a better functional form, we might be able to reject one or both of these as suboptimal. Given that the gamma and power law models seem to be providing unrealistically low and unrealistically high predictions of old water contributions, it is likely that they bracket the true behavior. As Figures 4d and 4e show, these models produce nearly identical predictions about the contributions of the youngest water but diverge for older water. It may be useful to compare both approaches in future applications in order to get a sense of the structural uncertainty inherent in predictions of old water contributions.

6.2. The Need for Age-Dependent Uncertainty

Ultimately, the indeterminacy mentioned above must be addressed through data and improved methods for integrating the data with the model in a way that accommodates uncertainty. Indeed, it might be best to go beyond current approaches based on ad hoc functional forms and calibrated parameters. Even where rigorous uncertainty analysis is used in the parameter estimation (e.g., Visser et al., 2019; Wilusz et al., 2017), these methods cannot tell us how uncertainty is distributed among the different age ranks in storage or how it changes in time. Thus, we risk being overconfident about the inferences that can be made regarding (for example) the contributions of old water to discharge at high flows.

It would be far better to let the data constrain only the portion of age selection that it is sensitive to and clearly determine when it can tell us little or nothing at all. This will likely only require adaptation of methods already developed for other purposes. Three components would be required:

- Do away with the constraining need to choose a functional form for Ω or f_T in favor of methods that either (a) test hypotheses, in the form of functions derived from physical insights about the internal controls on the flow and transport behavior, or (b) allow the data to determine the form of the data in a more flexible way.
- Place uncertainty bounds on the Ω or f_T that vary with age rank in storage and in time and show us the extent to which the data are able to provide insights about the turnover rate of water of different ages.
- Allow information from multiple tracers to be integrated together, each perhaps constraining different parts of the age-ranked storage—for example, stable isotope tracers constraining the contributions of 0- to 2-year old water, SF_6 constraining the contributions of water 2–20 years, and ^3H constraining contributions of older water (if possible). This was previously suggested in Rinaldo et al. (2015), and progress toward this goal can be found in Visser et al. (2019).

Massoudieh et al. (2014) has developed a method for steady-state TTD estimation that incorporates these abilities and that could be extended to SAS functions. Such methods could determine whether phenomena like the old water suppression observed in both examples above are an artifact of the choice of a gamma distribution or a physical reality. Without these rigorous steps, there is a risk that as the number of applications grow, the SAS approach will produce more heat than light, and the insights it generates could be regarded with suspicion.

Appendix A: The Catchment Sensitivity Function as Celerity

When a catchment sensitivity function or storage-discharge relation is used to represent catchment response, there is effectively no delay between the input of additional water to storage and the response at the outlet. In that sense, the celerity is effectively infinite. However, when we consider the propagation of variability through the system, a finite celerity may still be obtained. The celerity in that case represents the phase shift between the input (precipitation) and the output (discharge) response.

For example, consider the simple case where the catchment sensitivity function is given by

$$g(Q) = \frac{Q_{\text{ref}}}{s}\left(\frac{Q}{Q_{\text{ref}}}\right)^{b-1}, \tag{A1}$$

and this captures the response of the system through

$$\frac{\mathrm{d}Q}{\mathrm{d}t} = g(Q)\left(J(t) - Q(t)\right), \tag{A2}$$

as suggested by Kirchner (2009). Let us assume that the input $J(t)$ consists of periodic precipitation events occurring with period t_r. Figure 1 shows the solution (obtained numerically) when $J(t) = J_0(\sin(\pi t/t_r))^k$ with $J_0 = 1$, $t_r = 1$, $k = 10$, $b = 1.5$, $Q_{\text{ref}} = 1$, and $s = 0.05$, 0.1, and 0.2. The delay between the input and output is the result of the hydraulic response time implied by this model. Note that it is not a pure delay (translation in time), due to the nonlinearity of the model, and the presence of multiple frequencies of fluctuation in the input time series. We can nevertheless estimate the dominant phase shift and see that it is related to the hydraulic response time $1/g(Q)$.

To see this, we can linearize the model above around a characteristic discharge Q^*, so

$$g(Q) \approx g(Q^*) = \frac{Q_{\text{ref}}}{s}\left(\frac{Q^*}{Q_{\text{ref}}}\right)^{b-1}. \tag{A3}$$

Substituting this into (A2) gives a linear ordinary differential equation (ODE) that can be solved in the Fourier domain in the form of a product of the input $\tilde{J}(\omega)$ and a transfer function:

$$\tilde{Q}(\omega) = \tilde{J}(\omega)\frac{1}{1 + 2\pi i\omega/g(Q^*)} = \tilde{J}(\omega)\tilde{H}(\omega). \tag{A4}$$

The phase shift t_s induced by the transfer function at the base frequency $\omega = 1/t_r$ is then given by the negative argument of the transfer function:

$$t_s = \frac{t_r}{2\pi}\arctan\left(\frac{\text{Im}(\tilde{H}(\omega))}{\text{Re}(\tilde{H}(\omega))}\right) = \frac{t_r}{2\pi}\arctan\left(\frac{2\pi}{t_r g(Q^*)}\right). \tag{A5}$$

Figure 1b shows this relationship with $t_r = 1$, and Figure 1a shows the estimated phase shifts superimposed on the model results. For small values of $t_r g(Q^*)$, this shows that

$$t_s \approx 1/g(Q^*). \tag{A6}$$

A Taylor series expansion shows that this is true to $O((1/g(Q^*))^3)$ accuracy.

Acknowledgments
I would like to gratefully acknowledge the support of National Science Foundation grants EAR-1344664, CBET-1360415, and EAR-90072546. Thanks to Dano Wilusz, Minseok Kim, and Sihan Zhao for their thoughtful comments on the manuscript, as well as Ype van der Velde, Charles Luce, and an anonymous reviewer for their helpful feedback. No new data is presented in this paper. The SAS code can be obtained online (https://github.com/charman2/rsas).

References

Abramowitz, M., & Stegun, I. A. (1964). *Handbook of mathematical functions: With formulars, graphs, and mathematical tables* (Vol. 55). New York: Dover Publications.

Ajami, N. K., Duan, Q., & Sorooshian, S. (2007). An integrated hydrologic Bayesian multimodel combination framework: Confronting input, parameter, and model structural uncertainty in hydrologic prediction. *Water Resources Research*, *43*, 655. https://doi.org/10.1029/2005WR004745

Benettin, P., Kirchner, J. W., Rinaldo, A., & Botter, G. (2015). Modeling chloride transport using travel time distributions at Plynlimon, Wales. *Water Resources Research*, *51*, 3259–3276. https://doi.org/10.1002/2014WR016600

Benettin, P., Rinaldo, A., & Botter, G. (2013). Kinematics of age mixing in advection-dispersion models. *Water Resources Research*, *49*, 8539–8551. https://doi.org/10.1002/2013WR014708

Benettin, P., Soulsby, C., Birkel, C., Tetzlaff, D., Botter, G., & Rinaldo, A. (2017). Using SAS functions and high-resolution isotope data to unravel travel time distributions in headwater catchments. *Water Resources Research*, *53*, 1864–1878. https://doi.org/10.1002/2016WR020117

Beven, K. (2006). Searching for the Holy Grail of scientific hydrology: $Q_t = H(\underset{\leftarrow}{S}, \underset{\leftarrow}{R}, \Delta t)A$ as closure. *Hydrology and Earth System Sciences*, *10*(5), 609–618.

Beven, K. J. (2012). *Rainfall-runoff modelling*. The Primer: John Wiley & Sons.

Birkel, C., & Soulsby, C. (2016). Linking tracers, water age and conceptual models to identify dominant runoff processes in a sparsely monitored humid tropical catchment. *Hydrological Processes*, *30*(24), 4477–4493.

Birkel, C., Soulsby, C., & Tetzlaff, D. (2015). Conceptual modelling to assess how the interplay of hydrological connectivity, catchment storage and tracer dynamics controls nonstationary water age estimates. *Hydrological Processes*, *29*(13), 2956–2969.

Botter, G., Bertuzzo, E., & Rinaldo, A. (2011). Catchment residence and travel time distributions: The master equation. *Geophysical Research Letters*, *38*, L11403. https://doi.org/10.1029/2011GL047666

Brutsaert, W., & Nieber, J. L. (1977). Regionalized drought flow hydrographs from a mature glaciated plateau. *Water Resources Research*, *13*, 637–643.

Clark, M. P., Slater, A. G., Rupp, D. E., Woods, R. a., Vrugt, J. A., Gupta, H. V., et al. (2008). Framework for Understanding Structural Errors (FUSE): A modular framework to diagnose differences between hydrological models. *Water Resources Research*, *44*, W00B02. https://doi.org/10.1029/2007WR006735

Danckwerts, P. V. (1953). Continuous flow systems: Distribution of residence times. *Chemical Engineering Science*, *2*(1), 1–13.

Danesh-Yazdi, M., Klaus, J., Condon, L. E., & Maxwell, R. M. (2018). Bridging the gap between numerical solutions of travel time distributions and analytical storage selection functions. *Hydrological Processes*, *32*(8), 1063–1076.

Dralle, D. N., Hahm, W. J., Rempe, D. M., Karst, N. J., Thompson, S. E., & Dietrich, W. E. (2018). *Quantification of the seasonal hillslope water storage that does not drive streamflow* (Vol. 32, pp. 1978–1992).

Dralle, D. N., Karst, N. J., Charalampous, K., Veenstra, A., & Thompson, S. E. (2017). Event-scale power law recession analysis: Quantifying methodological uncertainty. *Hydrology and Earth System Sciences*, *21*(1), 65–81.
Dralle, D., Karst, N., & Thompson, S. E. (2015). a, b careful: The challenge of scale invariance for comparative analyses in power law models of the streamflow recession. *Geophysical Research Letters*, *42*, 9285–9293. https://doi.org/10.1002/2015GL066007
Farmer, D., Sivapalan, M., & Jothityangkoon, C. (2003). Climate, soil, and vegetation controls upon the variability of water balance in temperate and semiarid landscapes: Downward approach to water balance analysis. *Water Resources Research*, *39*(2), 1035. https://doi.org/10.1029/2001WR000328
Haitjema, H. M. (1995). On the residence time distribution in idealized groundwatersheds. *Journal of Hydrology*, *172*(1), 127–146.
Harman, C. J. (2015). Time-variable transit time distributions and transport: Theory and application to storage-dependent transport of chloride in a watershed. *Water Resources Research*, *51*, 1–30. https://doi.org/10.1002/2014WR015707
Harman, C. J., & Kim, M. (2014). An efficient tracer test for time-variable transit time distributions in periodic hydrodynamic systems. *Geophysical Research Letters*, *41*, 1567–1575. https://doi.org/10.1002/2013GL058980
Harman, C. J., & Sivapalan, M. (2009). A similarity framework to assess controls on shallow subsurface flow dynamics in hillslopes. *Water Resources Research*, *45*, W01417. https://doi.org/10.1029/2008WR007067
Harman, C. J., Sivapalan, M., & Kumar, P. (2009). Power law catchment-scale recessions arising from heterogeneous linear small-scale dynamics. *Water Resources Research*, *45*, W09404. https://doi.org/10.1029/2008WR007392
Harman, C. J., Ward, A. S., & Ball, A. (2016). How does reach-scale stream-hyporheic transport vary with discharge? Insights from rSAS analysis of sequential tracer injections in a headwater mountain stream. *Water Resources Research*, *52*, 7130–7150. https://doi.org/10.1002/2016WR018832
Hrachowitz, M., Savenije, H., Bogaard, T. A., Tetzlaff, D., & Soulsby, C. (2013). What can flux tracking teach us about water age distribution patterns and their temporal dynamics? *Hydrology and Earth System Sciences*, *17*(2), 533–564.
Jothityangkoon, C., Sivapalan, M., & Farmer, D. L. (2001). Process controls of water balance variability in a large semi-arid catchment: Downward approach to hydrological model development. *Journal of Hydrology*, *254*(1-4), 174–198.
Kim, M., Pangle, L. A., Cardoso, C., Lora, M., Volkmann, T. H. M., Wang, Y., et al. (2016). Transit time distributions and StorAge Selection functions in a sloping soil lysimeter with time-varying flow paths: Direct observation of internal and external transport variability. *Water Resources Research*, *52*, 7105–7129. https://doi.org/10.1002/2016WR018620
Kirchner, J. W. (2003). A double paradox in catchment hydrology and geochemistry. *Hydrological Processes*, *17*(4), 871–874.
Kirchner, J. W. (2009). Catchments as simple dynamical systems: Catchment characterization, rainfall-runoff modeling, and doing hydrology backward. *Water Resources Research*, *45*, W02429. https://doi.org/10.1029/2008WR006912
Kirchner, J. W. (2016). Aggregation in environmental systems—Part 2: Catchment mean transit times and young water fractions under hydrologic nonstationarity. *Hydrology and Earth System Sciences*, *20*(1), 299–328.
Kirchner, J. W., Feng, X., & Neal, C. (2000). Fractal stream chemistry and its implications for contaminant transport in catchments. *Nature*, *403*(6769), 524–527.
Klaus, J., Chun, K. P., McGuire, K. J., & McDonnell, J. J. (2015). Temporal dynamics of catchment transit times from stable isotope data. *Water Resources Research*, *51*, 4208–4223. https://doi.org/10.1002/2014WR016247
Klaus, J., & McDonnell, J. J. (2013). Hydrograph separation using stable isotopes: Review and evaluation. *Journal of Hydrology*, *505*, 47–64.
Lehmann, P., Hinz, C., Mcgrath, G., Tromp-van Meerveld, H. J., & McDonnell, J. J. (2007). Rainfall threshold for hillslope outflow: An emergent property of flow pathway connectivity. *Hydrology and Earth System Sciences*, *11*(2), 1047–1063.
Massoudieh, A., Visser, A., Sharifi, S., & Broers, H. P. (2014). A Bayesian modeling approach for estimation of a shape-free groundwater age distribution using multiple tracers. *Applied Geochemistry*, *50*, 252–264.
McDonnell, J. J., & Beven, K. (2014). Debates—The future of hydrological sciences: A (common) path forward? A call to action aimed at understanding velocities, celerities and residence time distributions of the headwater hydrograph. *Water Resources Research*, *50*, 5342–5350. https://doi.org/10.1002/2013WR015141
McDonnell, J. J., McGuire, K. J., Aggarwal, P., Beven, K. J., Biondi, D., Destouni, G., et al. (2010). How old is streamwater? Open questions in catchment transit time conceptualization, modelling and analysis. *Hydrological Processes*, *24*(12), 1745–1754.
McGuire, K. J., DeWalle, D. R., & Gburek, W. J. (2002). Evaluation of mean residence time in subsurface waters using oxygen-18 fluctuations during drought conditions in the mid-Appalachians. *Journal of Hydrology*, *261*(1-4), 132–149.
McGuire, K., & McDonnell, J. J. (2006). A review and evaluation of catchment transit time modeling. *Journal of Hydrology*, *330*(3-4), 543–563.
Meals, D. W., Dressing, S. A., & Davenport, T. E. (2010). Lag time in water quality response to best management practices: A review. *Journal of Environment Quality*, *39*(1), 85–96.
Neal, C., & Rosier, P. T. W. (1990). Chemical studies of chloride and stable oxygen isotopes in two conifer afforested and moorland sites in the British uplands. *Journal of Hydrology*, *115*(1-4), 269–283.
Pangle, L. A., Kim, M., Cardoso, C., Lora, M., Meira Neto, A. A., Volkmann, T. H. M., et al. (2017). The mechanistic basis for storage-dependent age distributions of water discharged from an experimental hillslope. *Water Resources Research*, *53*, 2733–2754. https://doi.org/10.1002/2016WR019901
Remondi, F., Kirchner, J. W., Burlando, P., & Fatichi, S. (2018). Water flux tracking with a distributed hydrological model to quantify controls on the spatiotemporal variability of transit time distributions. *Water Resources Research*, *54*, 3081–3099. https://doi.org/10.1002/2017WR021689
Rinaldo, A., Benettin, P., Harman, C. J., Hrachowitz, M., McGuire, K. J., van der Velde, Y., et al. (2015). Storage selection functions: A coherent framework for quantifying how catchments store and release water and solutes. *Water Resources Research*, *51*, 4840–4847. https://doi.org/10.1002/2015WR017273
Rodhe, A., Nyberg, L., & Bishop, K. (1996). Transit times for water in a small till catchment from a step shift in the oxygen 18 content of the water input. *Water Resources Research*, *32*(12), 3497–3511.
Rodriguez, N. B., McGuire, K. J., & Klaus, J. (2018). Time-varying storage—Water age relationships in a catchment with a Mediterranean climate. *Water Resources Research*, *54*, 3988–4008. https://doi.org/10.1029/2017WR021964
Rupp, D. E., & Selker, J. S. (2005). Drainage of a horizontal Boussinesq aquifer with a power law hydraulic conductivity profile. *Water Resources Research*, *41*, W11422. https://doi.org/10.1029/2005WR004241
Rupp, D. E., & Selker, J. S. (2006). On the use of the Boussinesq equation for interpreting recession hydrographs from sloping aquifers. *Water Resources Research*, *42*, W12421. https://doi.org/10.1029/2006WR005080
Schmadel, N. M., Ward, A. S., & Wondzell, S. M. (2017). Hydrologic controls on hyporheic exchange in a headwater mountain stream. *Water Resources Research*, *53*, 6260–6278. https://doi.org/10.1002/2017WR020576

Sivapalan, M. (2005). Pattern, process and function: Elements of a unified theory of hydrology at the catchment scale. In M. G. Anderson (Ed.), *Encyclopedia of hydrological sciences* (pp. 193–219). John Wiley & Sons, Ltd.

Sklash, M. G., & Farvolden, R. N. (1979). The role of groundwater in storm runoff. *Journal of Hydrology*, *43*(1), 45–65.

Soulsby, C., Birkel, C., Geris, J., Dick, J., Tunaley, C., & Tetzlaff, D. (2015). Stream water age distributions controlled by storage dynamics and nonlinear hydrologic connectivity: Modeling with high-resolution isotope data. *Water Resources Research*, *51*, 7759–7776. https://doi.org/10.1002/2015WR017888

Spence, C. (2010). A paradigm shift in hydrology: Storage thresholds across scales influence catchment runoff generation. *Geography Compass*, *4*(7), 819–833.

Troch, P. A., & De Troch, F. P. (1993). Effective water table depth to describe initial conditions prior to storm rainfall in humid regions. *Water Resources Research*, *29*(2), 427–434.

Troch, P. A., Paniconi, C., & van Loon, E. E. (2003). Hillslope-storage Boussinesq model for subsurface flow and variable source areas along complex hillslopes: 1. Formulation and characteristic response. *Water Resources Research*, *39*(11), 1316. https://doi.org/10.1029/2002WR001730

Tunaley, C., Tetzlaff, D., Birkel, C., & Soulsby, C. (2017). Using high-resolution isotope data and alternative calibration strategies for a tracer-aided runoff model in a nested catchment. *Hydrological Processes*, *31*(22), 3962–3978.

van Huijgevoort, M. H. J., Tetzlaff, D., Sutanudjaja, E. H., & Soulsby, C. (2016). Using high resolution tracer data to constrain water storage, flux and age estimates in a spatially distributed rainfall-runoff model. *Hydrological Processes*, *30*(25), 4761–4778.

Van Meter, K. J., & Basu, N. B. (2015). Catchment legacies and time lags: A parsimonious watershed model to predict the effects of legacy storage on nitrogen export. *PLOS ONE*, *10*(5), e0125971.

van der Velde, Y., Heidbüchel, I., Lyon, S. W., Nyberg, L., Rodhe, A., Bishop, K., & Troch, P. A. (2014). Consequences of mixing assumptions for time-variable travel time distributions. *Hydrological Processes*, *29*(16), 3460–3474.

van der Velde, Y., Torfs, P. J. J. F., van der Zee, S. E. A. T. M., & Uijlenhoet, R. (2012). Quantifying catchment-scale mixing and its effect on time-varying travel time distributions. *Water Resources Research*, *48*, W06536. https://doi.org/10.1029/2011WR011310

Visser, A., Thaw, M., Deinhart, A., Bibby, R., Safeeq, M., Conklin, M., et al. (2019). Cosmogenic isotopes unravel the hydrochronology and water storage dynamics of the Southern Sierra Critical Zone. *Water Resources Research*, *55*, 1429–1450. https://doi.org/10.1029/2018WR023665

Ward, A. S., Schmadel, N. M., Wondzell, S. M., Gooseff, M. N., & Singha, K. (2017). Dynamic hyporheic and riparian flow path geometry through base flow recession in two headwater mountain stream corridors. *Water Resources Research*, *53*, 3988–4003. https://doi.org/10.1002/2016WR019875

Ward, A. S., Schmadel, N. M., Wondzell, S. M., Harman, C. J., Gooseff, M. N., & Singha, K. (2016). Hydrogeomorphic controls on hyporheic and riparian transport in two headwater mountain streams during base flow recession. *Water Resources Research*, *52*, 1479–1497. https://doi.org/10.1002/2015WR018225

Wilusz, D. C., Harman, C. J., & Ball, W. P. (2017). Sensitivity of catchment transit times to rainfall variability under present and future climates. *Water Resources Research*, *53*, 10231–10256. https://doi.org/10.1002/2017WR020894

Wittenberg, H. (1999). Baseflow recession and recharge as nonlinear storage processes. *Hydrological Processes*, *13*(5), 715–726.

Wittenberg, H., & Sivapalan, M. (1999). Watershed groundwater balance estimation using streamflow recession analysis and baseflow separation. *Journal of Hydrology*, *219*(1-2), 20–33.

Wondzell, S. M., Gooseff, M. N., & McGlynn, B. L. (2007). Flow velocity and the hydrologic behavior of streams during baseflow. *Geophysical Research Letters*, *34*, L24404. https://doi.org/10.1029/2007GL031256

Wondzell, S. M., Gooseff, M. N., & McGlynn, B. L. (2009). An analysis of alternative conceptual models relating hyporheic exchange flow to diel fluctuations in discharge during baseflow recession. *Hydrological Processes*, *24*(6), 686–694.

Yang, J., Heidbüchel, I., Musolff, A., Reinstorf, F., & Fleckenstein, J. H. (2018). Exploring the dynamics of transit times and subsurface mixing in a small agricultural catchment. *Water Resources Research*, *54*, 2317–2335. https://doi.org/10.1002/2017WR021896

Zimmer, M. A., & McGlynn, B. L. (2017). Time-lapse animation of hillslope groundwater dynamics details event-based and seasonal bidirectional stream–groundwater gradients. *Hydrological Processes*, *31*(10), 1983–1985.